Port of Gladstone
Gatcombe and Golding Cutting
Channel Duplication Project

Environmental Impact Statement

Gladstone Ports Corporation
Growth, Prosperity, Community.

aurecon

11

Climate and climate change assessment

Contents

11 Climate and climate change assessment

11.1 Chapter purpose

The purpose of this chapter is to describe the climatic conditions that apply to the Project and the Project impact areas. This includes likely changing climate patterns, the risks of climate change on construction and operation, and the identification of mitigation and adaptation strategies to be implemented. Elements of the climate and climate change assessment include:

- Describing the existing climate of the Gladstone region, including historical data, climate drivers and extreme events (refer Section 11.3)
- Identification of climate change projections for key climate variables with the potential to impact on the Project (refer Sections 11.4 and 11.5)
- Assessment of the potential impacts of changing climate and weather patterns on the construction and operational phases of the Project (refer Section 11.6)
- Identification of mitigation measures and adaptation strategies to be implemented to minimise the potential climate change impacts on the Project (refer Section 11.7)
- Assessment of the risks associated with climate change impacts taking into account the implementation of mitigation measures and adaptation strategies (refer Section 11.8).

The climate and climate change assessment also informs the Project description and other impact assessment chapters in the EIS, including:

- Project description (Chapter 2)
- Hydrodynamics and sedimentation (Chapter 7)
- Water quality (Chapter 8)
- Nature conservation (Chapter 9)
- Hazard and risk (Chapter 20)
- Cumulative impact assessment (Chapter 21).

11.2 Methodology

11.2.1 Elements of the climate risk management process

The climate and climate change assessment for the Project forms a critical feature of climate risk management, as discussed in Australia/New Zealand AS/NZS ISO 31000:2009 Risk management—Principles and guidelines (Australian Standard 2013a).

Elements of the climate risk management process include:

- Identification of the objectives, including goals, values and imperative with respect to climate change and the adaptation of settlements and infrastructure
- Establishment of the climate change context, including definition of greenhouse gas emissions scenarios, future time slices, relevant climate variables and selection of data. This element includes determining the necessity of engaging specific impact studies based on findings.
- Establishment of interdependencies with external factors, which may include intangible and tangible context (e.g. social and cultural, political, financial, economic), as well as infrastructure critical to the development. This element also includes long term plans and identification of trends, taking into account any relevant changes (e.g. demographics).

- Characterisation of the internal context pertinent to the GPC and the Project. This element encompasses all aspects of the GPC's culture, and would cover governance arrangements, standards and guidelines, strategies, assets and resources, and all information, including information channels.
- Establishment of the context of risk management process which includes the definition of the assets (settlement or infrastructure) being considered, the potential hazards, and the boundaries of the risk assessment (i.e. temporal, spatial and scope of responsibility)
- Definition of the risk criteria, which should be used to evaluate the significance of risk and should be consistent with the risk criteria used for other forms of risks. This can be defined in terms of measures of consequences, likelihood, and evaluation for prioritisation.

The climate risk assessment was conducted in a three-part process, including:

- Climate assessment
- Climate change assessment
- Climate change impact assessment.

The methodology implemented for each of these parts is provided below.

11.2.2 Climate assessment

A climate assessment was conducted to establish existing climate conditions of the Gladstone region. The climate assessment included a discussion of the sensitivity of the construction and operation phases, which identified critical climate parameters to infrastructure and proposed activities of the proposed development. The climate assessment included establishment of baseline climate, extreme events, and conditions with respect to the main drivers for variability.

The climate assessment considered climatic conditions within the Gladstone region in the context of its location and unique geographic features. Historical data from 1954 to 2018 collected by the BoM at its meteorological monitoring station located at Radar Hill were used as the basis in characterising long term rainfall, temperature, humidity, wind speed, wind direction and sea level pressure in the region.

The main driver for climate variability in the region has been identified as the El Niño–Southern Oscillation (ENSO) cycles, modulated by the phase of the Pacific Decadal Oscillation (PDO). These are shown to have the greatest effect on seasonal rainfall patterns, the frequency of warm nights and the frequency of tropical cyclones. There does not appear to be a strong climate signal evident from individual extreme events. The analysis suggests that rainfall and temperature, particularly overnight temperatures, are the most likely climate variables to be impacted by climate change.

Average summer rainfall is shown to double during La Niña/Cool PDO compared to the summer average. An increase of a similar magnitude is seen in the average number of high rain days shifting from 4.5 days to 9.7 days. This pattern is also shown in the frequency of tropical cyclones where a 23% increase in the number of tropical cyclones passing within 400km of Gladstone has been shown.

The frequency of warm nights was also shown to be influenced by the ENSO/PDO phases showing a decrease in warm nights under La Niña/Cool PDO conditions and an increase in the number of warm nights under El Niño/Warm PDO and Neutral/Warm PDO.

Sea level rise has been found to be occurring gradually since 1880, with a more rapid increase observed in the 20th century. Rosslyn Bay is the closest station that is part of the Australian Baseline Sea Level Monitoring Project (ABSLMP) managed by the BoM. Sea level rise and wave height data from 1992 to 2018 shows that while trends observed during the short time period are subtle and not easily defined, an upward trend can be observed in the maximum monthly sea level indicator.

11.2.3 Climate change assessment

The assessment of climate change aims to determine and quantify future climate conditions with respect to established baseline conditions. Climate change is determined by comparing outputs from global and/or regional models, as well as statistically downscaled projections with established baselines for the period relevant to the project. Climate projection is discussed in more detail in Section 11.4.1. This section includes discussions of scenarios, models and period of modelling.

Climate change was addressed on a regional context, to provide additional perspective to the projected local changes. A more localised assessment for the East Coast cluster (where Gladstone is located) was conducted using the online tool Climate Change in Australia (CCIA). CCIA is discussed in further detail in Sections 11.4.2.

This assessment was conducted with particular focus on climate projections from models running the most conservative Representative Concentration Pathways (RCP) scenario. RCP8.5 scenario, similar in underlying assumptions to the A2 Special Report on Emissions Scenarios (SRES) scenario, which assumes a ‘business as usual’ trend in population growth, economic growth, and demand for energy. Construction activities for the Project are planned to occur from 2020 out to 2026 or later. The climatic period 2050 (30 years centred on 2050), was selected as the period of interest, to provide a conservative outlook for the anticipated construction period of the Project. Climate projections for 2030 and 2090, based on CCIA analysis is also considered where appropriate. Climate change projections for 2030 and 2050 provide an indication of the potential effects of climate change on the construction phase of the Project compared to 2090 projections that can be used to guide the design and future operations of Project-related infrastructure and future land uses.

Rainfall and temperature were identified as the critical variables likely to be affected by climate change, hence, these variables form the basis of the assessment. Other climate variables available from the dataset were also analysed and presented for completeness. Limited data for extreme events were also presented, where available.

The methodology adopted for the risk assessment is provided in Section 11.8.

11.3 Existing environment

Gladstone (latitude: -23.25, longitude: 151.29) is located in the Gulf of Capricorn. The region is classified as sub-tropical with no dry season under the BoM modified Koeppen Classification. The climate is characterised by hot and humid summers and warm winters. Unlike other tropical and sub-tropical locations, it does not experience a distinct dry season. This is likely due to the influence of the southeast trade winds, which provide a ready source of moisture from the Coral Sea.

This section provides a summary of historical climate data and subsequently considers the relationship between key climate parameters and climate drivers relevant to the Gladstone region.

11.3.1 Historical climate data

Meteorological monitoring data from the BoM station at Radar Hill (refer Table 11.1) has been used to characterise long term rainfall, temperature, humidity, wind speed, wind direction and sea level pressure in the Gladstone region. Prior to 1994, observations at Radar Hill were manually recorded by a dedicated observer at 9.00am and 3.00pm, the daily minimum and maximum temperatures and the daily total rainfall up to 9.00am were also recorded. The amount of data available for each variable can vary, the analysis states the valid time period for each variable when it is presented. In July 1994, an automatic weather station was installed at Radar Hill replacing manual observations with recorded measurements.

Table 11.1 Bureau of Meteorology Radar Hill observation and automatic weather station location

Radar Hill	Commenced	Last record	Latitude	Longitude	Elevation
Daily manual observations	1957	1993	-23.86	151.26	75m
Half hourly automatic weather station records	1994	2018	-23.86	151.26	75m

11.3.2 Climate drivers

11.3.2.1 El Niño Southern Oscillation

The ENSO consists of the El Niño, La Niña and neutral phases, each with its own effect on climate. In the neutral phase, trade winds blow east to west across the surface of the tropical Pacific Ocean, bringing warm moist air and warmer surface waters towards the western Pacific. Under El Niño conditions these trade winds weaken and the sea surface temperatures (SST) in the central and eastern tropical Pacific increase causing a shift in rainfall from the western Pacific (eastern Australia) to the central and eastern tropical Pacific (off the coast of South America). La Niña conditions are the opposite; the trade winds intensify causing SST in the western tropical Pacific Ocean to increase and shifting the rainfall pattern further into eastern Australia (BoM 2005).

El Niño and La Niña events tend to begin in spring, mature during summer then begin to decay in autumn of the following year, with the event generally ending in the winter of that following year. As such, any analysis of ENSO variations excludes the spring season as it is the build-up and decay period, commonly referred to in the literature as the transition period, and not representative of ENSO-related effects. The ENSO cycle tends to last between 6 and 18 months where the phase is determined by the 30 and 90-day rolling average of the Southern Oscillation Index (SOI). A persistent SOI of -7 is considered to be an El Niño, while persistent +7 SOI is La Niña and the values between -7 and +7 are Neutral.

11.3.2.2 Pacific Decadal Oscillation

The PDO overlays the intra-seasonal variability defined by the ENSO pattern with a decadal pattern that can last between 20 and 40 years. The PDO exhibits a warm phase and a cool phase and can have an influence on Pacific Ocean cyclone activity, droughts and flooding in the Pacific basin and land surface temperature patterns. There is some evidence that the phase of the PDO can either intensify or diminish the effects of the ENSO cycle, such that when both ENSO and PDO are in phase, for example La Niña and Cool PDO, the effects of the La Niña conditions can be enhanced and conversely La Niña under the influence of Warm PDO may diminish the La Niña conditions.

Figure 11.1 shows the SOI and PDO from 1903 to 2018, only two complete cycles of the PDO have been identified in the past century. The last warm phase is thought to have ended sometime in the mid-1990s; this analysis has assumed that period to be 1977 to 1996. The present period 1997 onwards is currently undefined and will remain indeterminate for at least another 10 to 20 years.

Table 11.2 shows the frequency of La Niña, El Niño and neutral ENSO conditions for all years that coincide with the cool and a Warm PDO. The frequency of El Niño and La Niña events appears to be moderated by the PDO where La Niña events are more frequent during Cool PDO and El Niño events are more frequent during Warm PDO. The frequency of neutral years; however, remains relatively the same across all PDO phases.

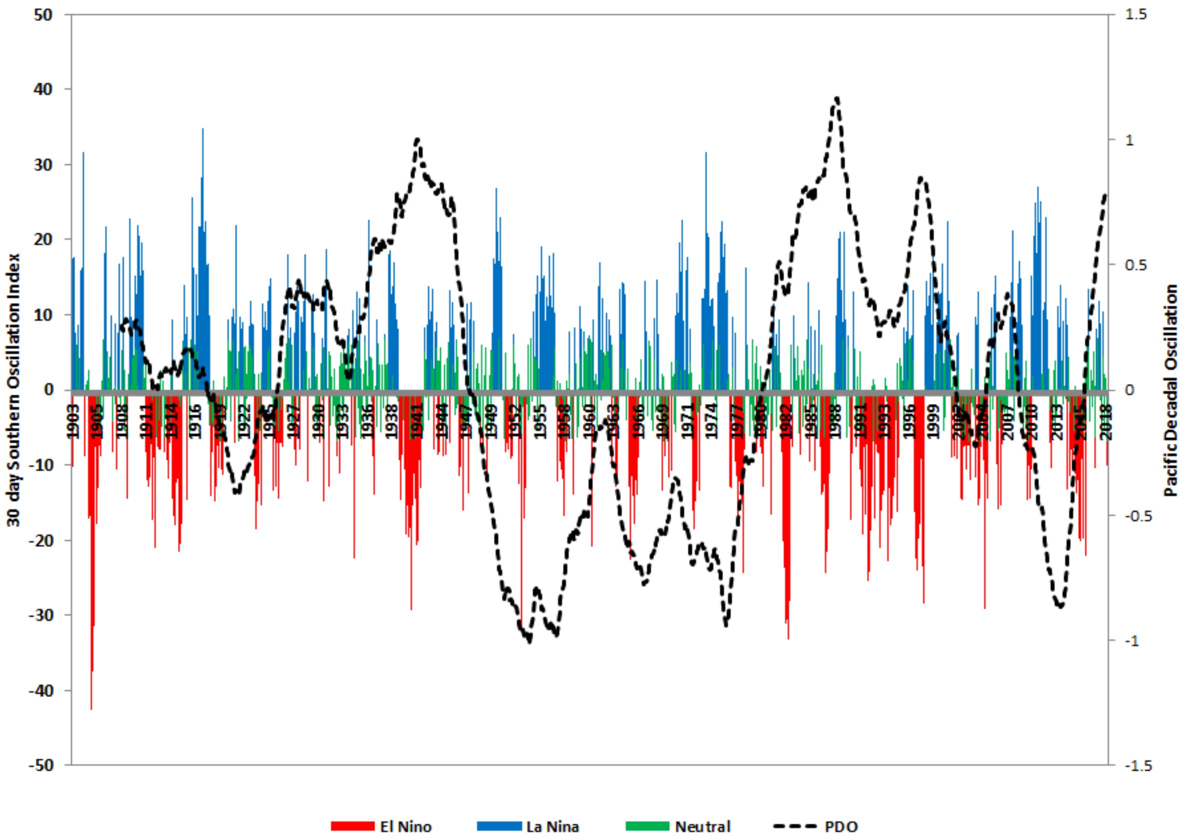

Figure 11.1 Southern Oscillation Index and Pacific Decadal Oscillation for the period 1903 to 2018

Table 11.2 El Niño and La Niña periods by Pacific Decadal Oscillation phase from 1903 to 2017

PDO Phase	Decadal period	El Niño	La Niña	Neutral
Cool	1890 to 1924*	27%	31%	42%
Warm	1925 to 1946	22%	22%	56%
Cool	1947 to 1976	17%	29%	54%
Warm	1977 to 1996	34%	13%	53%
Unknown	1997 to 2018	25%	29%	46%

Table note:

* High quality data is only available from 1900 onwards

11.3.3 Rainfall

This section provides a summary of historical rainfall followed by analysis of rainfall patterns against a background of relevant climate drivers. Extreme rainfall events are also considered separately.

11.3.3.1 Historical rainfall

Total annual rainfall for the years 1958 to 2017 is shown in Figure 11.2. The years 1957, 1993, 1994, 2003 and 2007 have been excluded from the annual totals as data for these years are incomplete. The annual average rainfall in Gladstone is 892 millimetres (mm) with a maximum annual total of 1,732mm (1971) and a minimum annual total of 432.5mm (1965).

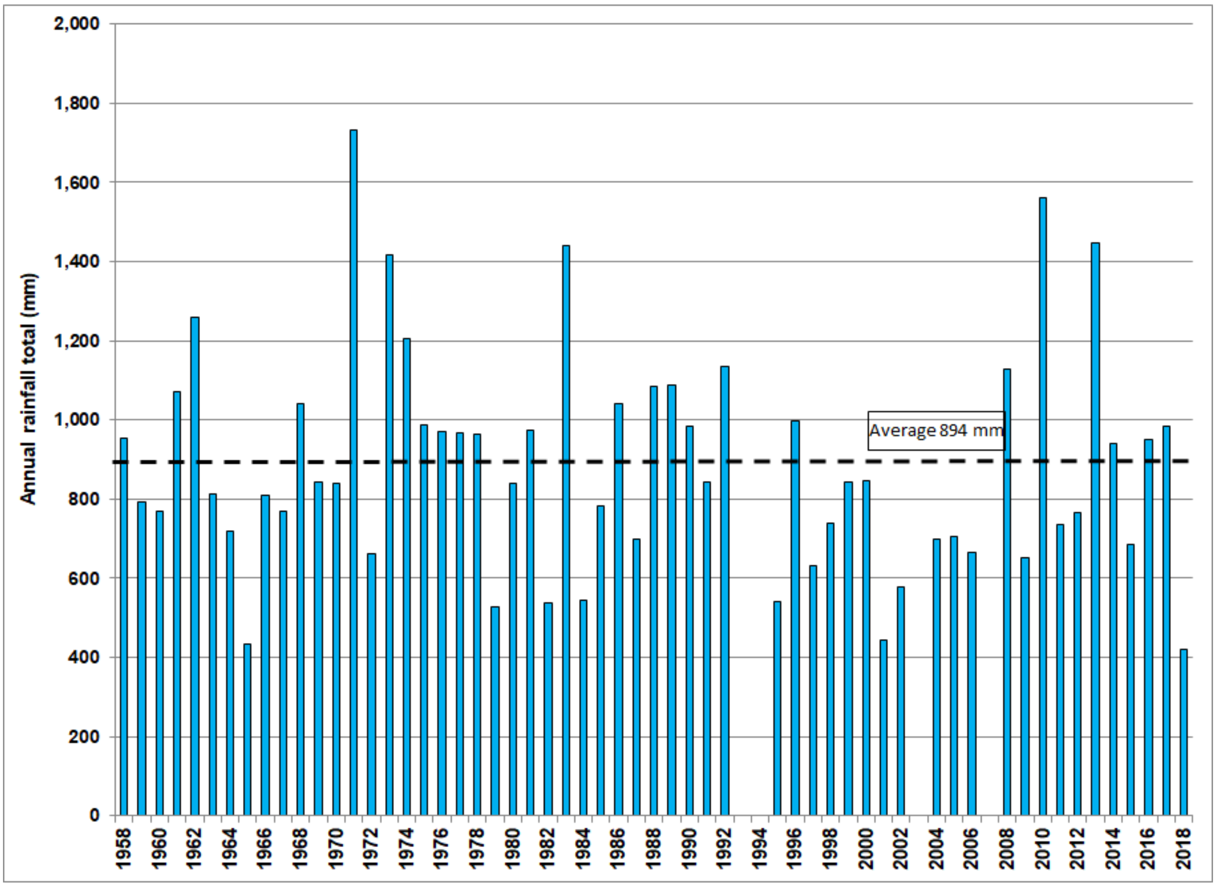

Figure 11.2 Annual total rainfall at Radar Hill for the years 1958 to 2018

As there is no distinct dry season, the seasonal analysis has been conducted using three-month periods consisting of:

- Summer: December, January, February
- Autumn: March, April, May
- Winter: June, July, August
- Spring: September, October, November.

Figure 11.3 shows the seasonal distribution of rainfall at Radar Hill for the period 1957 to spring 2018. The mean total rainfall peaks during the summer months and is at its lowest during winter.

The summer period accounts for 47% of the annual mean rainfall while winter only accounts for 12%. The shoulder seasons of spring and autumn account for 18% and 23%, respectively. The average summer rainfall is 411mm; this is higher than the maximum total rainfall recorded in winter and spring and just below the 95th percentile autumn rainfall (493mm).

Rain days are defined as a 24-hour period with greater than or equal to 0.2mm of rain, while a high rain day is defined as a 24-hour period with greater than or equal to 25mm of rain. Figure 11.4 and Figure 11.5 show the seasonal average number of rain days and high rain days at Radar Hill for the period 1957 to spring 2018. Summer is the season with the highest average number of rain days (34) and high rain days (4.4). Autumn displays the second highest average rain days (26) and high rain days (2.3).

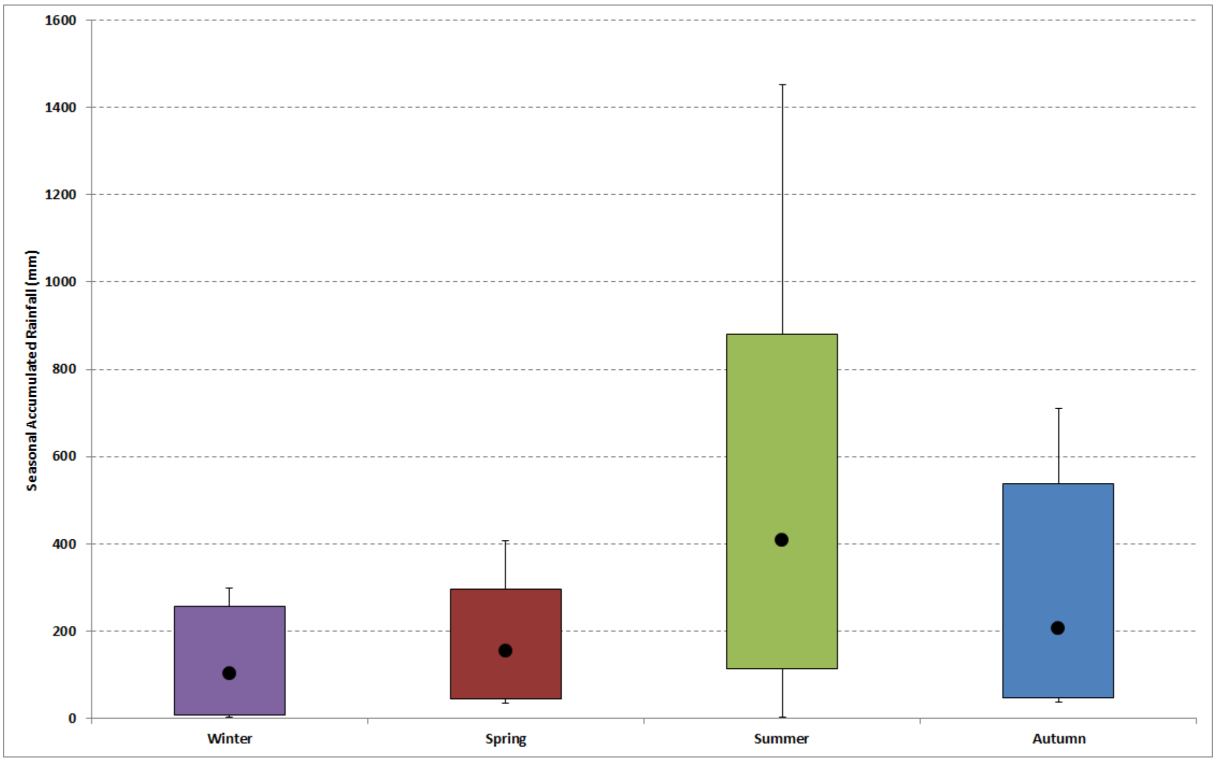

Figure 11.3 Season rainfall at the Radar Hill monitoring station for the period 1957 to spring 2018

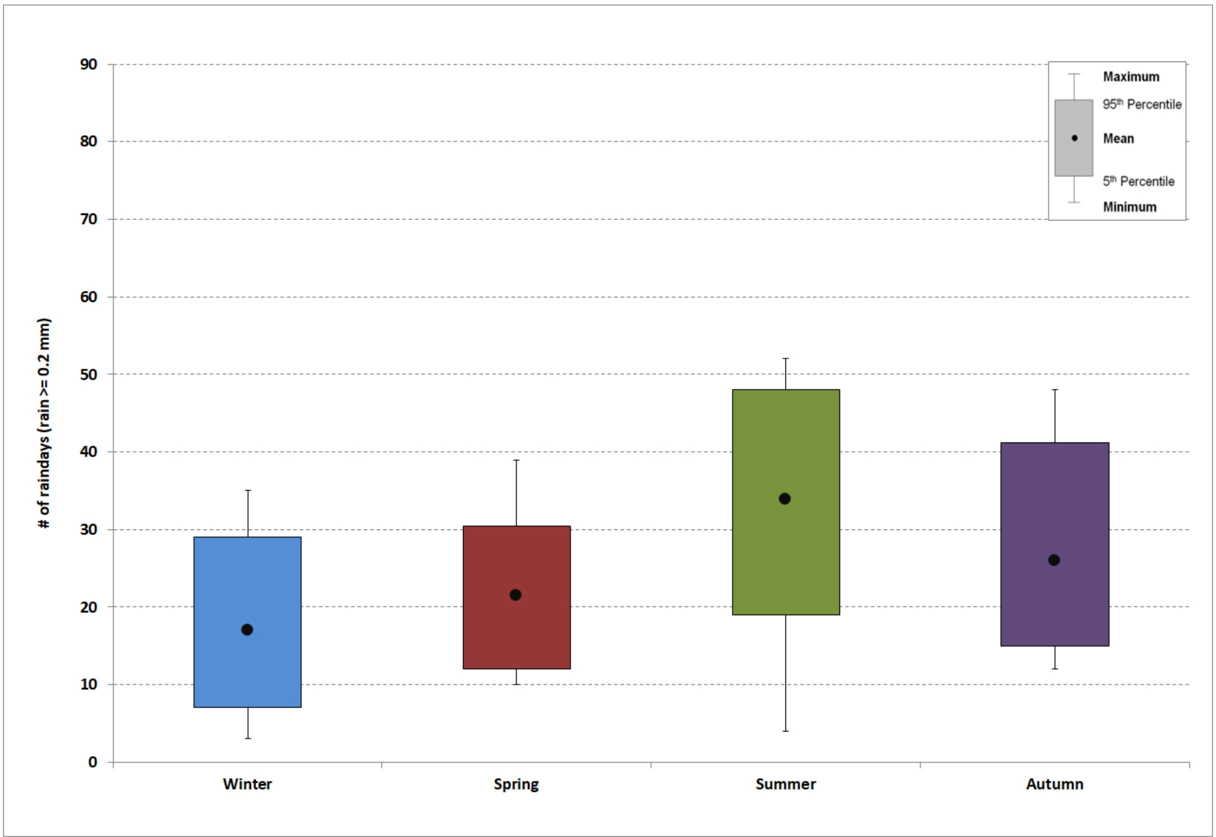

Figure 11.4 Seasonal average number of rain days (> 0.2mm) at Radar Hill 1957 to spring 2018

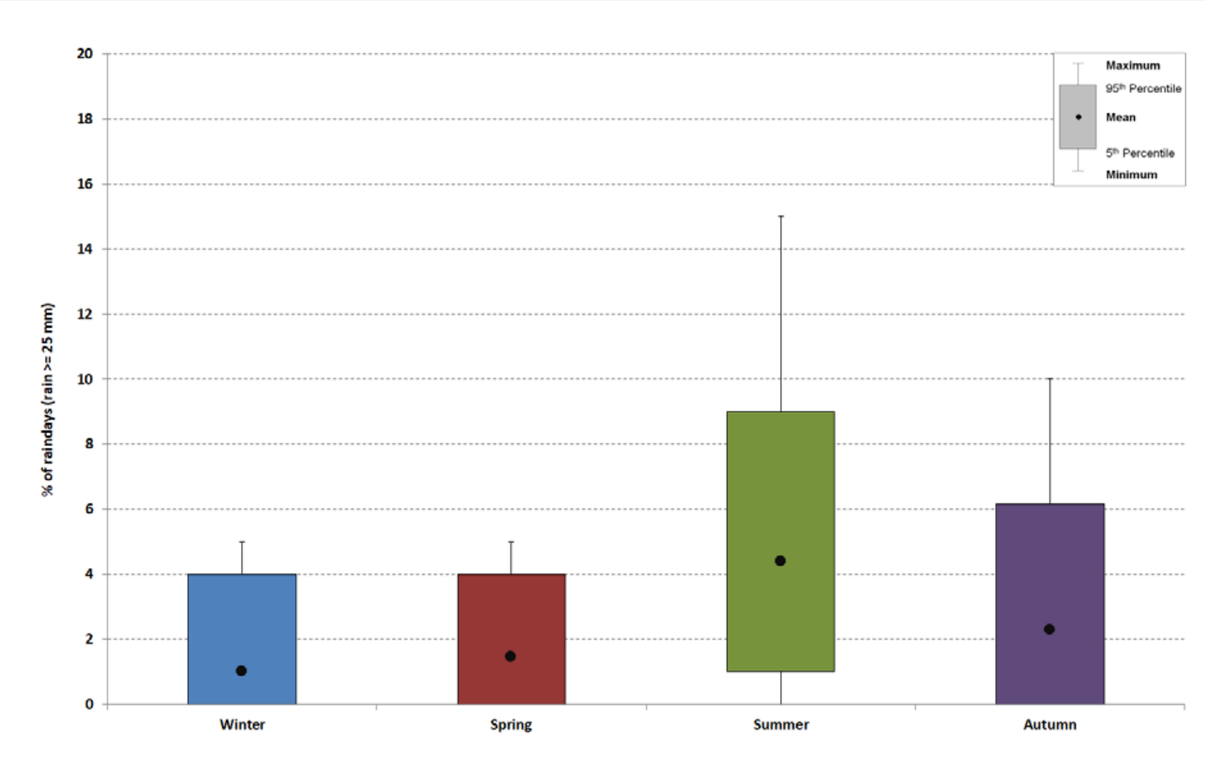

Figure 11.5 Seasonal average number of high rain days (> 25mm) at Radar Hill 1957 to spring 2018

11.3.3.2 Climate drivers

El Niño–Southern Oscillation/Pacific Decadal Oscillation rainfall

The spring and winter seasonal rainfall shows little variation when filtered by ENSO and PDO phases, with La Niña conditions showing a slightly higher average and range of total rainfall than El Niño and Neutral conditions regardless of PDO phase (refer Figure 11.6). Conversely, the summer season shows a dramatic variation between ENSO and PDO phases. This is expressed clearly during a La Niña and Cool PDO (refer Figure 11.6). Under these conditions the average summer rainfall is 735mm, equivalent to the annual average for all years on record and more than double the average summer rainfall of 408mm. The range has also expanded with a 95th percentile rainfall total of 1,334mm and 5th percentile of 195mm compared to the average summer range of 766mm (95th percentile) and 114mm (5th percentile).

Autumn also shows an increase in its range from Warm PDO to Cool PDO; however, its average remains the same. This may be an artefact of natural variability and not an influence of the climate ENSO/PDO interaction itself.

Figure 11.7 shows the seasonal average number of rain days by ENSO and PDO phases. The average is comparable between phases with typical seasonal pattern of more rain days in summer than in winter evident regardless of ENSO or PDO phases.

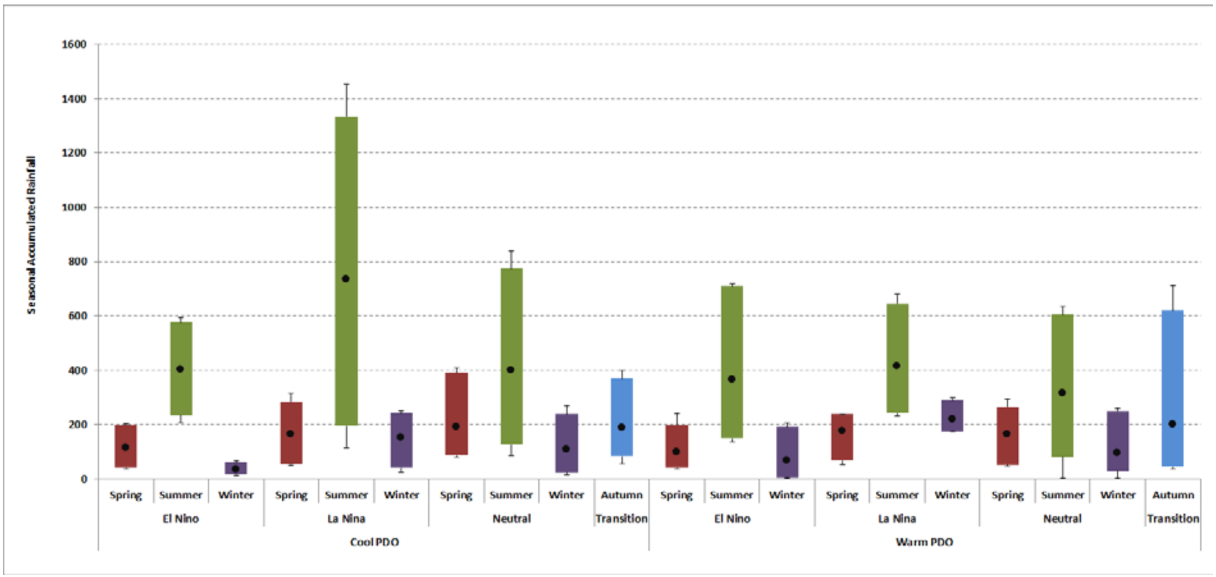

Figure 11.6 **Seasonal average accumulated rainfall (mm) by El Niño–Southern Oscillation and Pacific Decadal Oscillation phases**

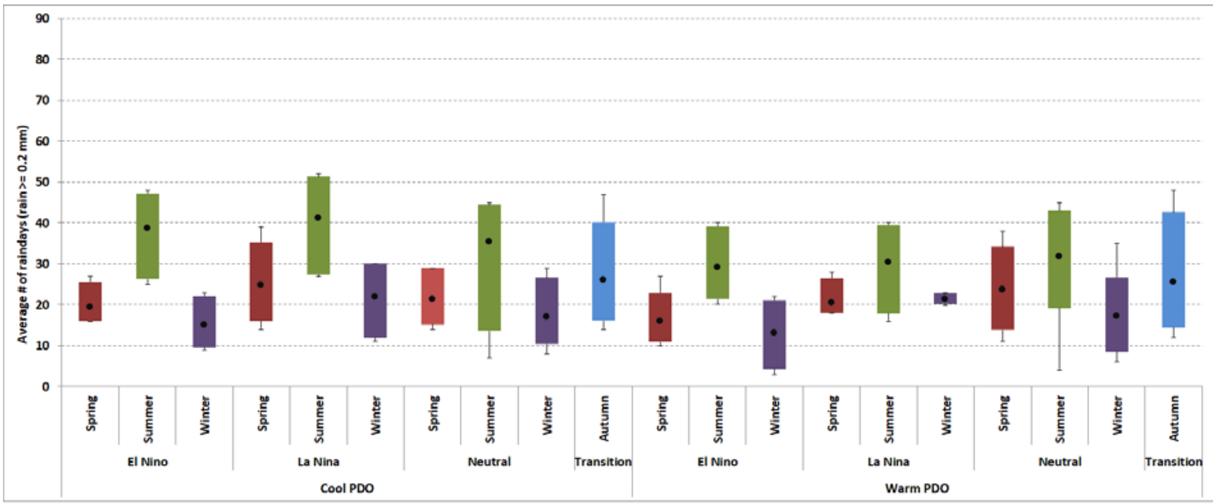

Figure 11.7 **Seasonal average number of rain days (rain >= 0.2mm) by El Niño–Southern Oscillation and Pacific Decadal Oscillation phases**

Figure 11.8 shows the seasonal average number of high rain days by ENSO and PDO phases. The influence of La Niña and Cool PDO phase on the number of high rain days in summer is evident. The average number of rain days above 25mm shifts to 7.1 under these conditions compared to the average summer value of 4.4 and the average summer 95th percentile of 8.0 (refer Table 11.3).

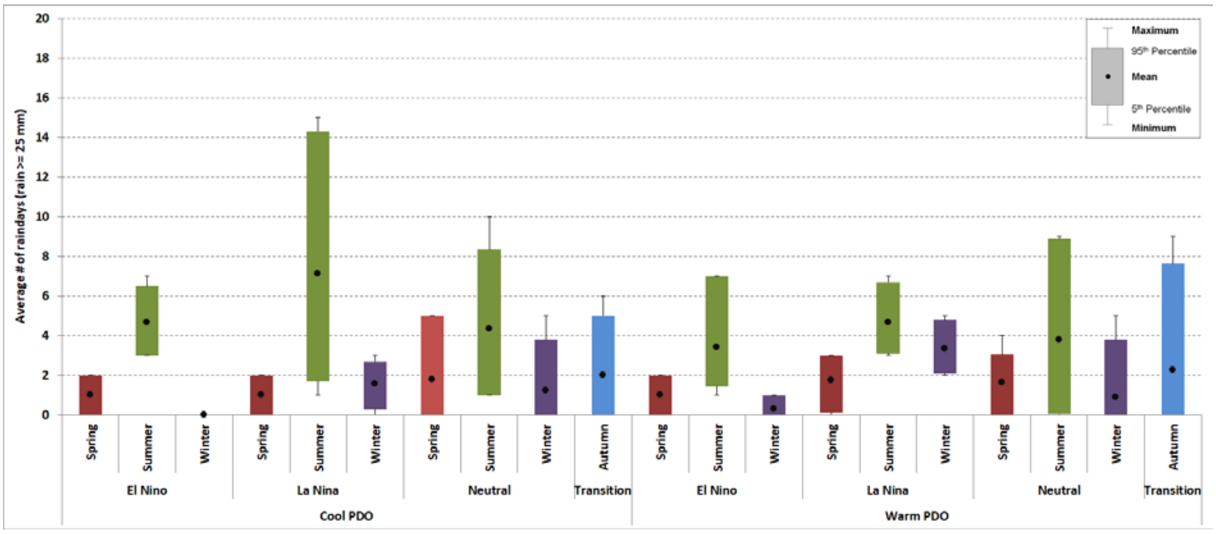

Figure 11.8 Seasonal average number of high rain days (rain >= 25mm) by El Niño–Southern Oscillation and Pacific Decadal Oscillation phases

Table 11.3 Number of rain days greater than 25mm for all summer periods and Cool Pacific Decadal Oscillation/La Niña summer periods

Summer climate	Number of rain days >= 25mm		
	5th percentile	Average	95th percentile
All years	1	4.4	8.0
Cool PDO/La Niña	1.7	7.1	14.3

Extreme rainfall

Table 11.4, Table 11.5 and Table 11.6 show the rainfall extremes recorded at Radar Hill for the period 1957 to 2018. The highest monthly rainfall totals and highest daily rainfall totals all occur during the summer months of December, January and February.

The highest monthly total was recorded in January 2013 with 841.4mm. This month also recorded the highest daily rainfall total of 254.4mm on 25 January 2013. The extreme rainfall event coincided with the passage of Tropical Cyclone Oswald, where 819.8mm of rain was recorded over a four-day period (24 to 27 January 2013).

The second highest single rain day event occurred on 5 February 2003 and was associated with Tropical Cyclone Beni where 557mm of rain was recorded over a 3-day period (5 February to 7 February 2003). This, however, did not translate to the highest total February on record. The highest February total rainfall occurred in 1971 when 709mm was recorded the same year that the highest annual total rainfall of 1,732mm was recorded. February 1971 also experienced two tropical cyclones within 400km of Gladstone, Dora and Fiona. The month also recorded 20 rain days and eight rain days greater than 25mm.

The lowest monthly rainfall totals are predominantly in the winter months, although January 2017 saw the lowest total rainfall (0.0mm) of any of the summer months. The low rainfall totals tend to be associated with El Niño and Neutral ENSO phases, while the influence of the PDO appears to be less predominant.

Extremely high rainfall occurs predominantly during the Australian monsoon season (November to April) and can be associated with tropical cyclone activity. However, the data also shows that high rainfall events are not necessarily associated with tropical cyclones and can potentially occur at any time of the year. The ENSO/PDO interaction shows a greater influence on average rainfall while its influence on high rainfall events is currently inconclusive.

Table 11.4 Highest monthly rainfall recorded at Radar Hill 1957 to 2018

Month	Highest monthly rainfall (mm)	Date	ENSO	PDO
January	841.4	2013	Neutral	Undefined
February	709.8	1971	La Niña	Cool
March	370.6	2014	Neutral	Undefined
April	250.4	1990	Neutral	Warm
May	316.4	1983	El Niño	Warm
June	220.3	1967	Neutral	Cool
July	170.2	1973	El Niño	Cool
August	141.6	1998	El Niño	Undefined
September	130.2	2010	El Niño	Undefined
October	276.8	1975	La Niña	Cool
November	218.1	1961	Neutral	Cool
December	508.9	1962	Neutral	Cool

Table 11.5 Lowest monthly rainfall recorded at Radar Hill 1957 to 2018

Month	Lowest monthly rainfall (mm)	Date	ENSO	PDO
January	0	2017	El Niño	Undefined
February	2.2	2017	El Niño	Undefined
March	2.4	1995	El Niño	Warm
April	0	2017	El Niño	Undefined
May	0.2	1984	Neutral	Warm
June	0	1968	Neutral	Cool
July	0	2002	Neutral	Undefined
August	0	2013	Neutral	Undefined
September	0	2017	El Niño	Undefined
October	0.4	2006	Neutral	Undefined
November	1.4	1982	Neutral	Warm
December	0.4	2016	El Niño	Undefined

Table 11.6 Highest daily rainfall recorded at Radar Hill 1957 to 2018

Month	Highest daily rainfall (mm)	Date	ENSO	PDO	Tropical Cyclone within 400km radius
January	254.4	25 January 2013	Neutral	Undefined	Oswald
February	248	5 February 2003	El Niño	Undefined	Beni
March	156	22 March 2012	La Niña	Undefined	-
April	97.8	19 April 2011	La Niña	Undefined	-
May	178	14 May 1977	Neutral	Warm	-
June	94.8	11 June 2006	Neutral	Undefined	-
July	92.7	3 July 1964	El Niño	Cool	-
August	78.2	23 August 1988	El Niño	Warm	-

Month	Highest daily rainfall (mm)	Date	ENSO	PDO	Tropical Cyclone within 400km radius
September	75	30 September 1986	Neutral	Warm	-
October	149.4	7 October 1961	Neutral	Cool	-
November	88	9 November 1999	La Niña	Undefined	-
December	196	18 December 1988	El Niño	Warm	-

11.3.4 Temperature

This section provides a summary of historical temperatures followed by analysis of key temperature parameters against a background of relevant climate drivers. Extreme temperature events are also considered separately.

11.3.4.1 Historical temperature

The average daily temperature by season at Radar Hill for the period 1957 to 2018 is shown in Figure 11.10. Summer has the highest mean temperature of 26.7°C, followed by autumn and spring. Autumn has the largest range of mean daily temperatures, which is expected as it is the transition period from summer to winter.

The average maximum and minimum temperatures (Figure 11.10 and Figure 11.11) follow a similar pattern with summer showing the highest average maximum and minimum temperatures and autumn showing the largest range of temperatures. Table 11.7 shows the average number of days the daily minimum temperature is above 25°C (warm nights) and the daily maximum temperature is above 35°C (hot days) for each season. Summer is shown to have the highest average number of days for both criteria while autumn and spring have an average of less than 1 day.

Table 11.7 Average number of days the daily minimum temperature is above 25 °C and the daily maximum temperature is above 35°C

Season	Average number of days daily maximum temperature ≥ 35°c	Average number of days daily minimum temperature ≥ 25°c
Autumn	0.3	0.4
Spring	0.6	0.1
Summer	3.7	5.2
Winter	0.0	0.0

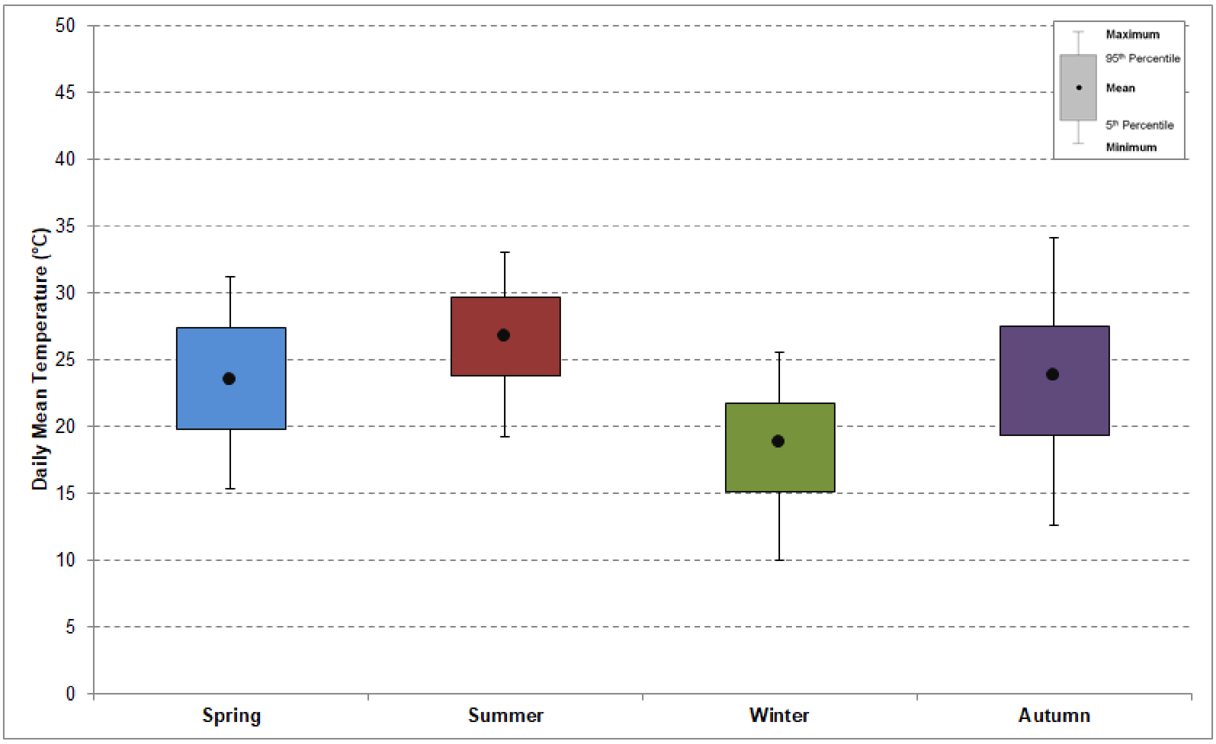

Figure 11.9 Daily average temperatures observed at Radar Hill for the period 1957 to spring 2018

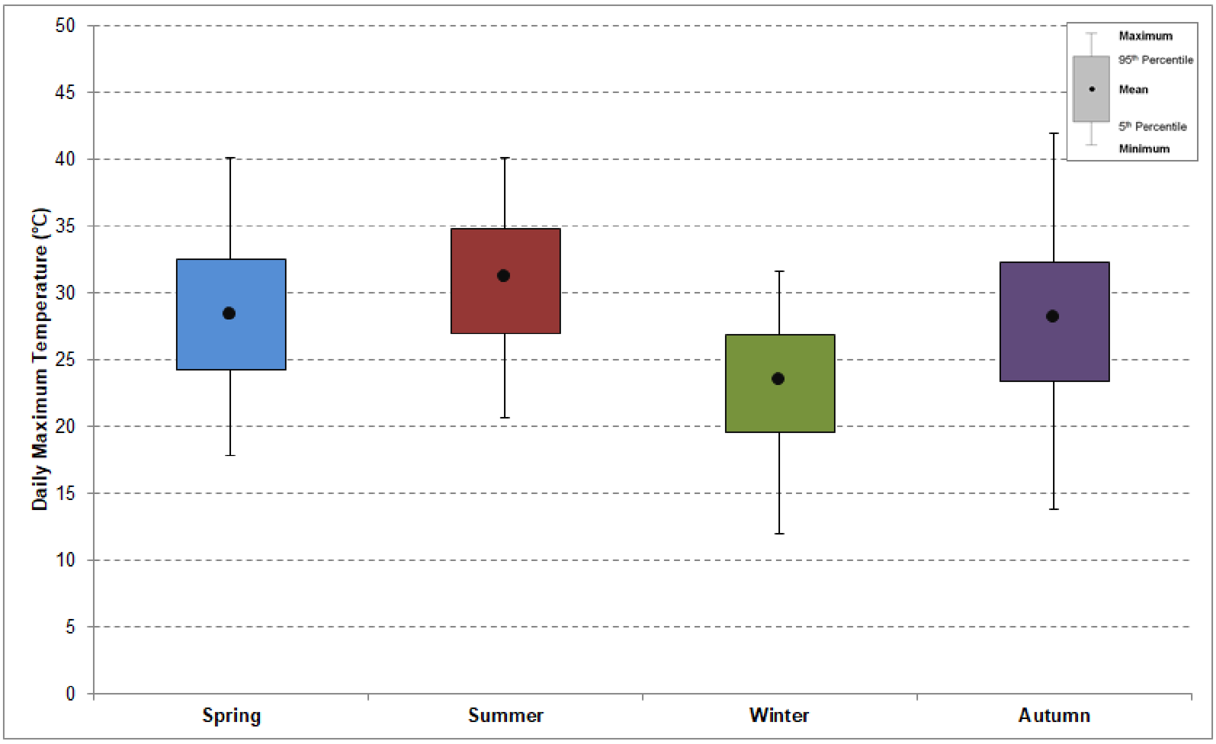

Figure 11.10 Daily maximum temperatures observed at Radar Hill for the period 1957 to spring 2018

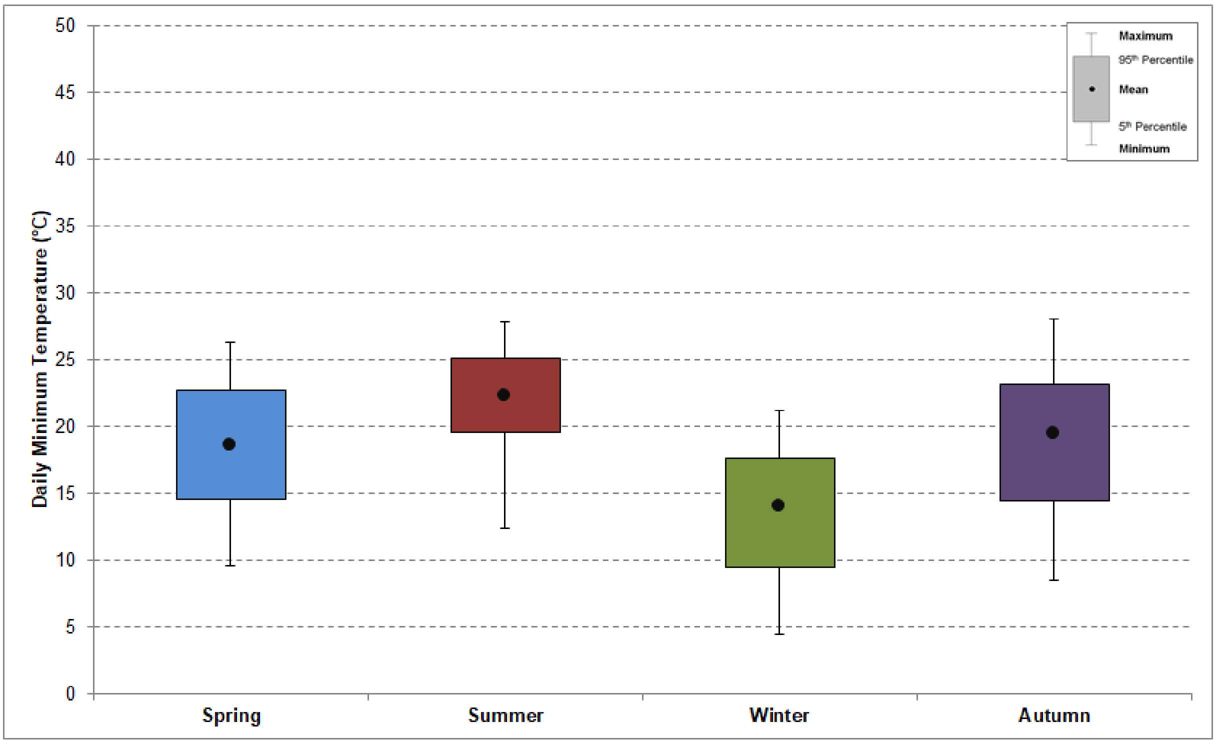

Figure 11.11 Daily minimum temperatures observed at Radar Hill for the period 1957 to spring 2018

11.3.4.2 Climate drivers

El Niño–Southern Oscillation/Pacific Decadal Oscillation temperature

The ENSO/PDO does not appear to have any influence on the mean, maximum or minimum temperatures recorded at Radar Hill (refer Figure 11.12, Figure 11.13 and Figure 11.14). The overriding seasonal variability remains consistent throughout the ENSO and PDO phases. The average number of hot days also shows little variation between ENSO and PDO phases. The largest variation is seen during summer under Neutral ENSO and Warm PDO where the number of days above 35°C is 4.7 compared to the average of 3.9. The largest reduction is seen during summer El Niño/Cool PDO conditions where the number of days drops to 2 (refer Figure 11.15 and Figure 11.16).

The average number of warm nights shows a stronger influence during summer under the ENSO/PDO phases. The La Niña/Cool PDO condition shows a drop in the number of warm nights to 2.1 compared to the average of 5.4 and the Neutral/Warm PDO sees an increase to 8.0 warm nights. There is also a small increase evident during El Niño/Warm PDO.

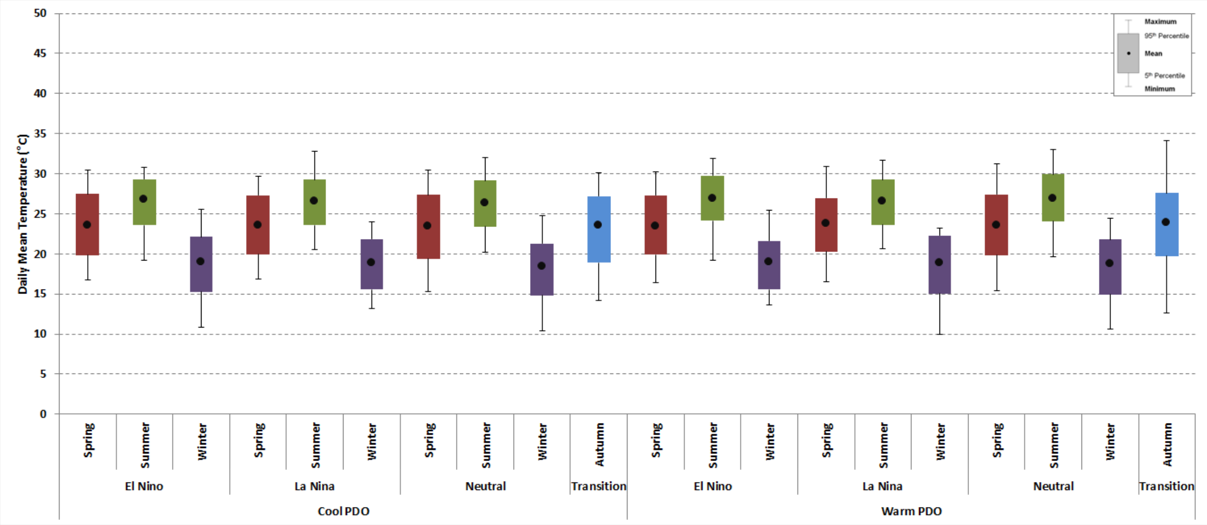

Figure 11.12 **Seasonal average temperature (°C) by El Niño–Southern Oscillation and Pacific Decadal Oscillation phases**

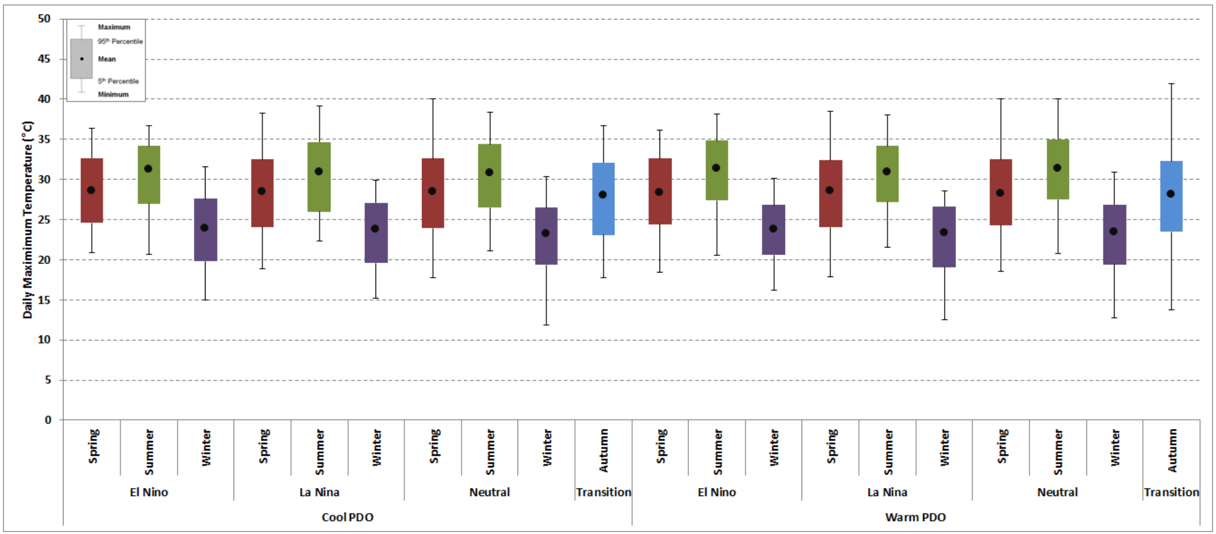

Figure 11.13 **Seasonal maximum temperature (°C) by El Niño–Southern Oscillation and Pacific Decadal Oscillation phases**

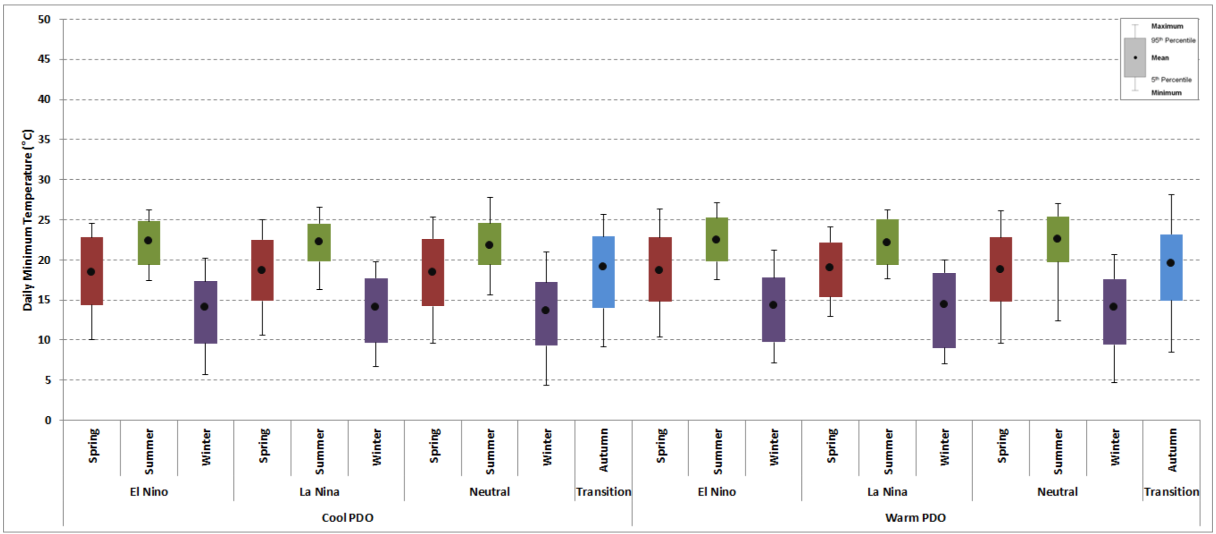

Figure 11.14 **Seasonal minimum temperature (°C) by El Niño–Southern Oscillation and Pacific Decadal Oscillation phases**

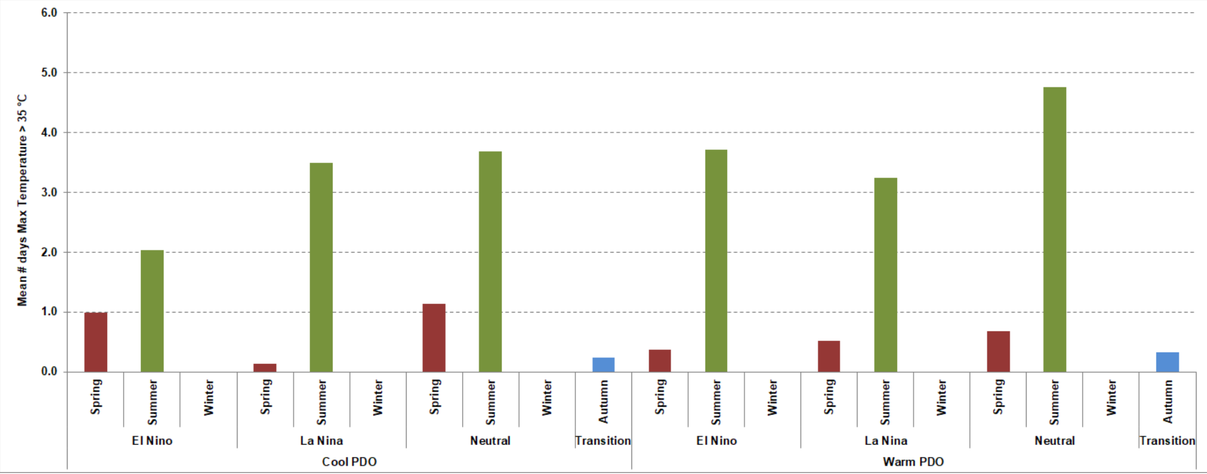

Figure 11.15 **Seasonal average number days maximum temperature is greater than 35°C by El Niño–Southern Oscillation and Pacific Decadal Oscillation phases**

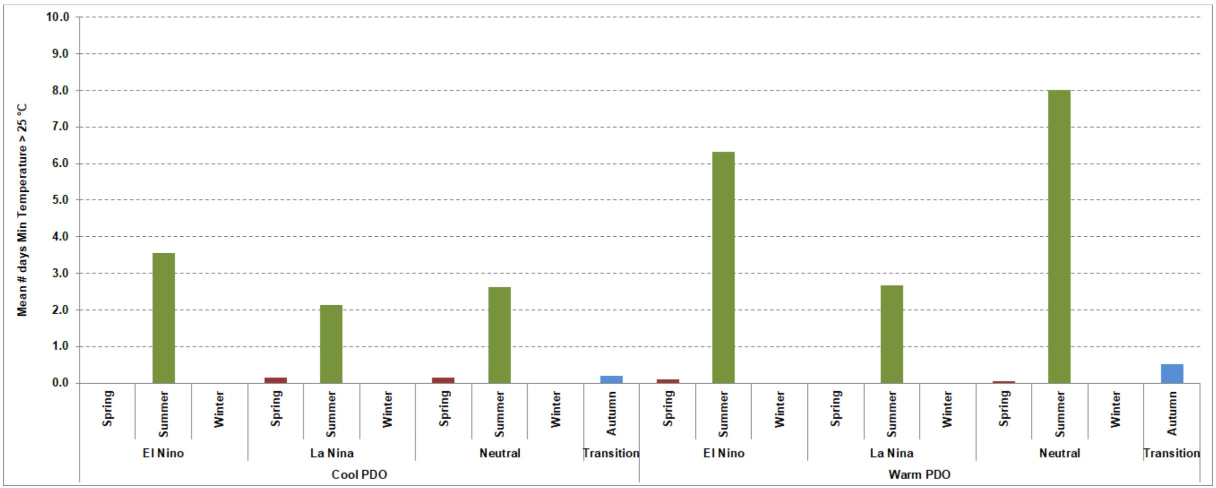

Figure 11.16 **Seasonal average number days minimum temperature greater than 25°C by El Niño–Southern Oscillation and Pacific Decadal Oscillation phases**

Extreme temperature

Temperature extremes for daily maximum and minimum temperatures are shown in Table 11.8 and Table 11.9. Daily maximum temperatures above 35°C have been recorded in each month from October through to March. The daily maximum temperature has never exceeded 35°C between April and September. Daily minimum temperatures above 25°C have been recorded in each month from November to April; this coincides with the Australian Monsoon season. The daily minimum temperature has never exceeded 25°C between April and September. There does not appear to be strong relationship between the ENSO/PDO phases and the extreme temperature events nor are they related to tropical cyclone activity with only Tropical Cyclone Dinah being within 400km of Gladstone when these records were set.

Table 11.8 Highest daily maximum temperatures reported by month at Radar Hill 1957 to 2018

Month	Highest temperature (°C)	Date	ENSO	PDO	Tropical Cyclone within 400km radius
January	38.3	30 January 1967	Neutral	Cool	Dinah
February	40.1	3 February 1990	Neutral	Warm	-
March	42	12 March 2007	El Nino	Undefined	-
April	34.4	2 April 2009	La Nina	Undefined	-
May	33.2	2 May 2016	El Nino	Undefined	-
June	29.7	17 June 2002	Neutral	Undefined	-
July	29.4	2 July 2009	La Nina	Undefined	-
August	31.6	30 August 2009	La Nina	Undefined	-
September	33.8	29 September 2017	El Nino	Undefined	-
October	40	31 October 1958	El Nino	Cool	-
November	40.1	18 November 1990	Neutral	Warm	-
December	39.8	8 December 1981	Neutral	Warm	-

Table 11.9 Highest daily minimum temperatures reported by month at Radar Hill 1957 to 2018

Month	Highest minimum temperature (°C)	Date	ENSO	PDO	Tropical Cyclone within 400km radius
January	27.1	12 January 1983	El Nino	Warm	-
February	27.0	1 February 2016	Neutral	Undefined	-
March	28.1	20 March 1995	El Nino	Warm	-
April	25.7	5 April 2006	Neutral	Undefined	-
May	22.6	2 May 1968	Neutral	Cool	-
June	21.2	17 June 2002	Neutral	Undefined	-
July	19.6	14 July 2012	La Nina	Undefined	-
August	20.2	26 August 2009	La Nina	Undefined	-
September	22.1	28 September 1997	Neutral	Undefined	-
October	23.7	28 October 2007	El Nino	Undefined	-
November	26.3	25 November 1987	Neutral	Warm	-
December	27.8	23 December 1958	El Nino	Cool	-

11.3.5 Wind speed and wind direction

This section provides a summary of historical wind speed and wind direction followed by analysis of wind characteristics against a background of relevant climate drivers. Extreme wind speed events are also considered separately.

11.3.5.1 Historical wind speed and wind direction

Features of the Gladstone region that affect the flow of winds include its coastal proximity, the large deep water harbour and elevated terrain around Mt Larcom. Seasonal variations in wind patterns are largely influenced by southeast trade winds with diurnal variations due to sea breezes resulting in a high percentage of easterly daytime winds.

Wind speed observations for the period 1968 to 2010 at 9.00am and 3.00pm are shown in Figure 11.17. The determination of mean daily diurnal wind speed on a monthly basis, for Radar Hill, was discontinued post-2010. The 9.00am wind speeds are seen to be on average 2m/s lower than the afternoon records. This is probably due to the initiation of a localised sea breeze circulation. The seasonal characteristic of the wind speeds is also evident with the highest winds occurring during the summer months, while the winter period is characterised by lower wind speeds and less variation between the morning and afternoon records.

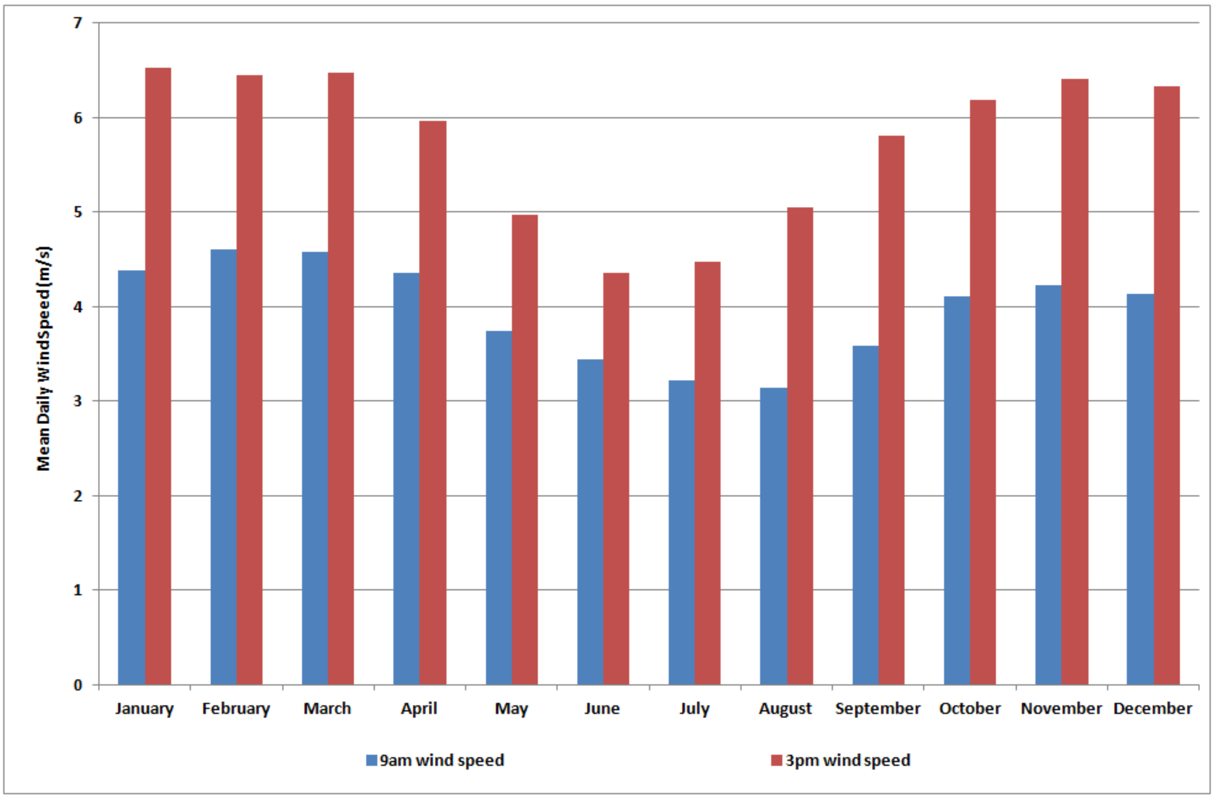

Figure 11.17 Mean monthly wind speed (m/s) at Radar Hill 1968 to 2010

The annual distribution of wind speed and direction at Radar Hill for the period January 1994 to December 2018 is presented as a wind rose diagram in Figure 11.18. The predominant winds at Radar Hill are from the northeast and southeast sector accounting for over 60% of all winds, this is largely driven by the southeast trade winds.

The seasonal distributions of wind speed and direction is presented in Figure 11.19. The southeast trade winds are evident throughout the year and dominate the summer, spring and autumn seasons.

Figure 11.20 shows the diurnal variation of the wind field at Radar Hill, again the southeast trade winds are evident as the dominant wind pattern. The swing from southeast in the morning hours to northeast in afternoon is driven by the heating of the land surface and the generation of a sea breeze circulation.

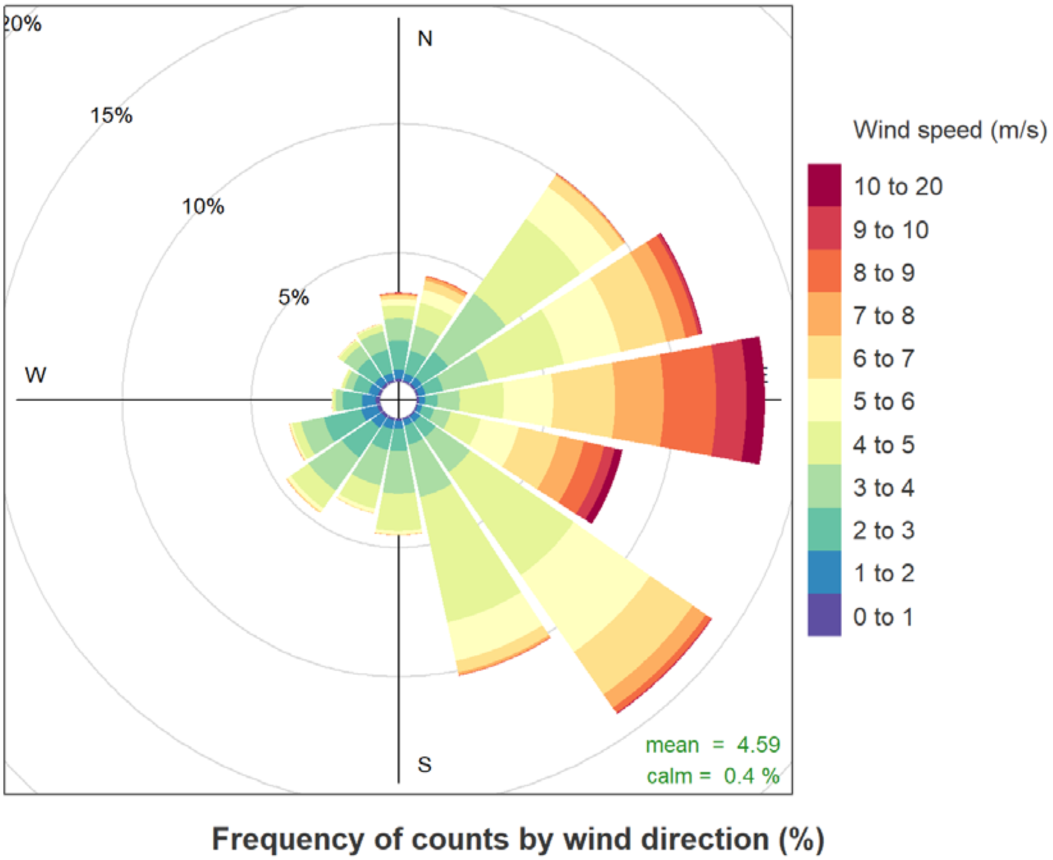

Figure 11.18 Annual distribution of wind speed and direction for Radar Hill (July 1994 to March 2018)

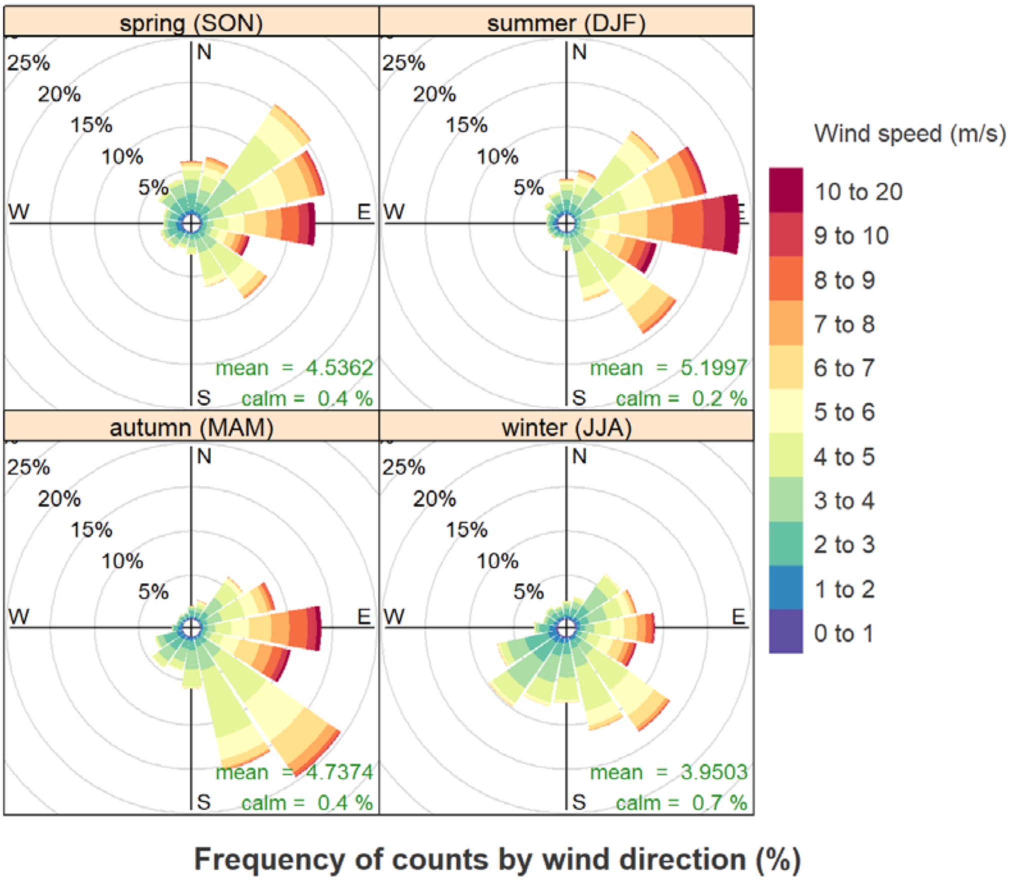

Figure 11.19 Seasonal distribution of wind speed and direction for Radar Hill (July 1994 to March 2018)

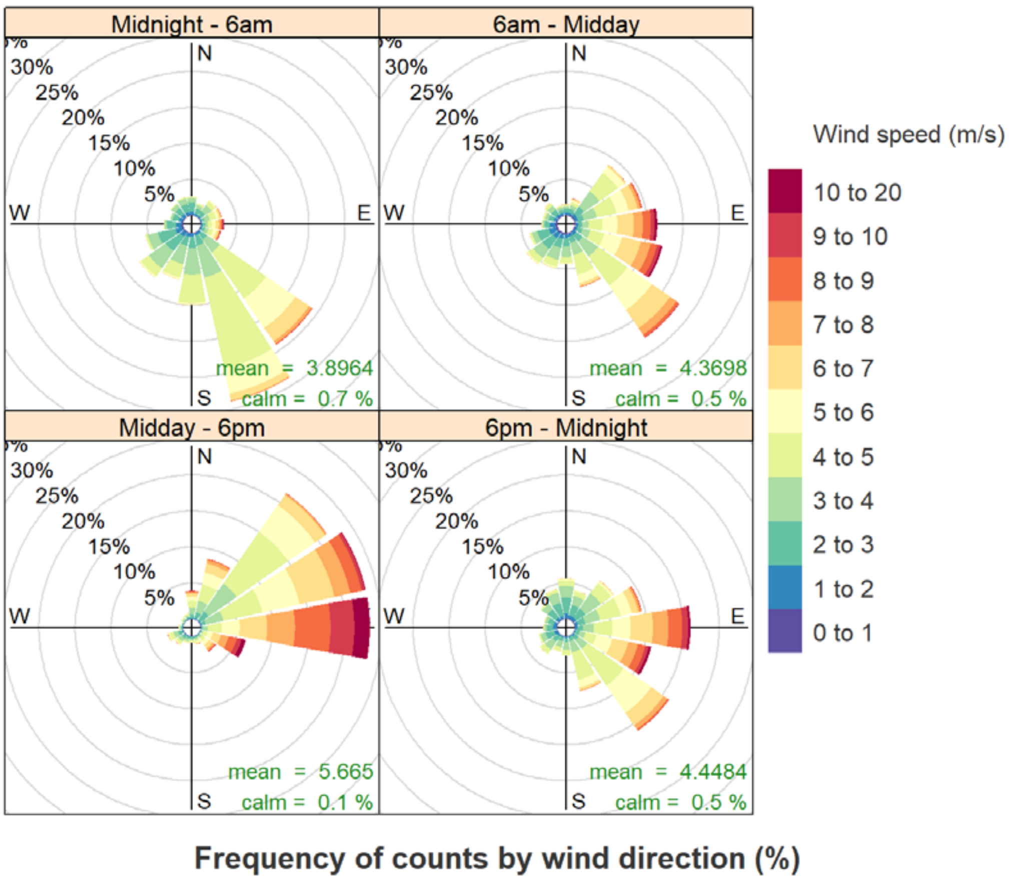

Figure 11.20 Diurnal distribution of wind speed and direction for Radar Hill (July 1994 to March 2018)

11.3.5.2 Climate drivers

El Niño–Southern Oscillation wind speed

This section discusses the results of the analysis for Gladstone Radar Hill station based on wind speed data collected from July 1994 to December 2018. The available data only covers the Warm PDO phase.

The range of seasonal average temperature by season and by ENSO phase is shown in Figure 11.21 and Figure 11.22, respectively. The consistency in ranges and minimal variability in mean wind speed values show that wind speeds are relatively unaffected by seasons or ENSO phase.

The data shows minimal occurrence of wind speeds greater than 15m/s. This only occurred four times in the dataset, and all these times occurred during summer.

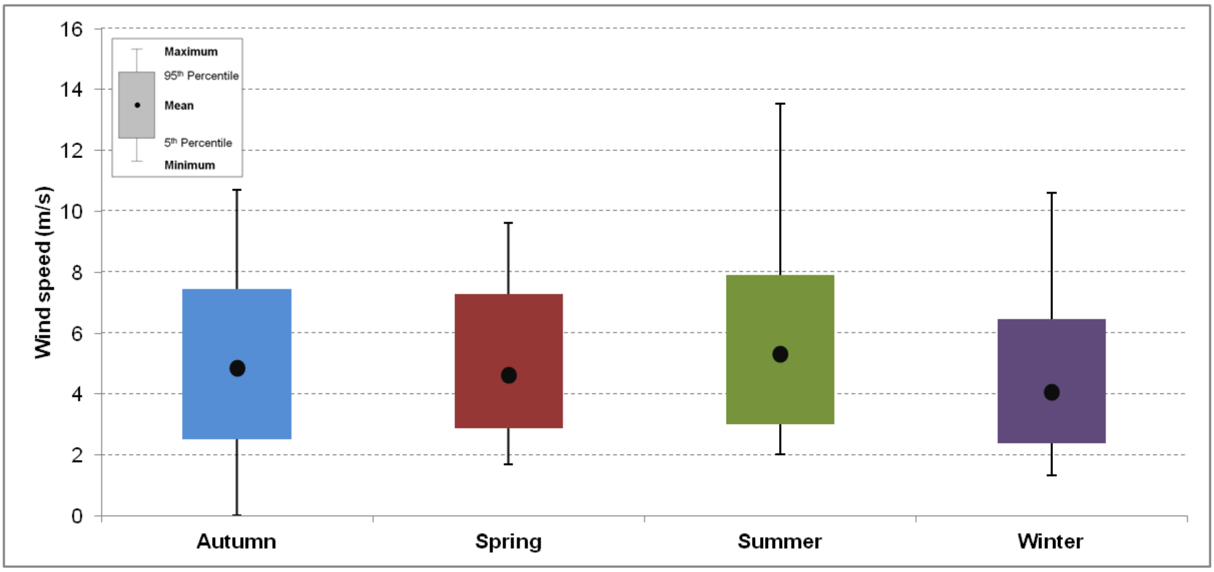

Figure 11.21 Seasonal wind speed (m/s)

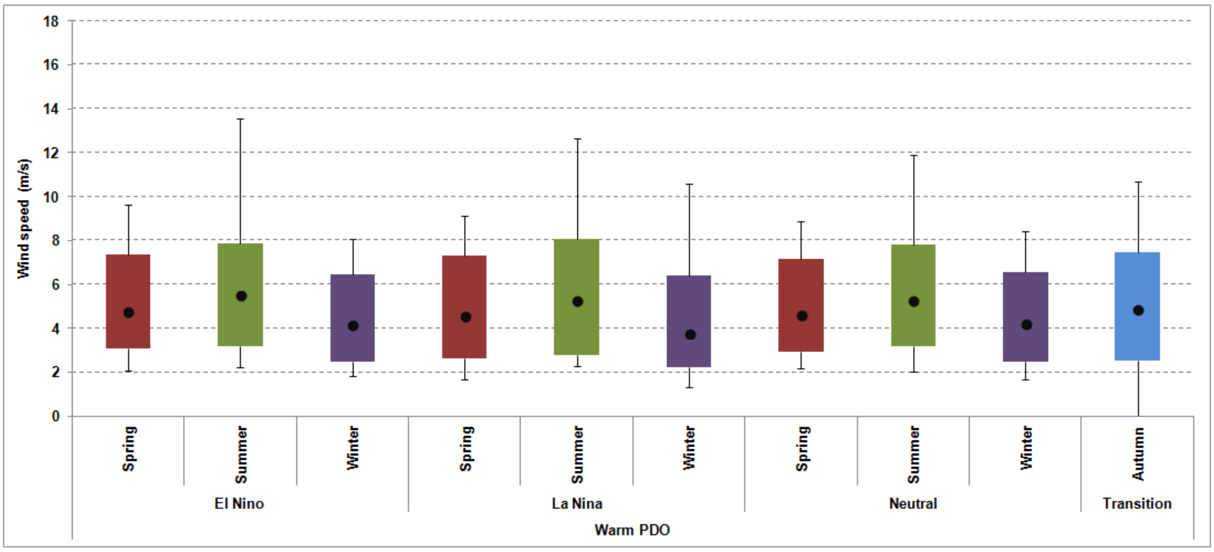

Figure 11.22 Seasonal wind speed (m/s) by El Niño–Southern Oscillation

Extreme wind speed

Table 11.10 shows the maximum wind gust recorded by month for the period 1968 to 2018. The day the maximum wind gust was recorded has been matched with the tropical cyclone subset for Gladstone and the name of the tropical cyclone has been identified. Six of the maximum wind gusts have been matched to the passing of tropical cyclones within 400km of Gladstone. The August, September and October maximum gusts cannot be attributed to tropical cyclones as none have been recorded during these months. The May, June and December maximum gusts also do not coincide with a tropical cyclone, even though tropical cyclones have been recorded during these months. This indicates that other meteorological situations such as storms and frontal systems can cause extreme wind conditions.

Table 11.10 Maximum wind gust speed by month for the period 1968 to 2018

Month	Maximum wind gust speed (km/h)	Date	ENSO	PDO	Tropical Cyclone
January	156	19 January 1976	La Nina	Cool	David
February	117	25 February 1980	Neutral	Warm	Simon
March	126	5 March 1976	La Nina	Cool	George
April	150	2 April 1972	La Nina	Cool	Emily
May	95	2 May 1983	El Nino	Warm	-
June	82	2 June 1973	El Nino	Cool	-
July	97	5 July 1973	El Nino	Cool	Unnamed
August	82	19 August 1982	Neutral	Warm	-
September	106	4 September 1984	Neutral	Warm	-
October	93	18 October 1975	La Nina	Cool	-
November	111	15 November 1969	Neutral	Cool	Unnamed
December	124	8 December 1982	Neutral	Warm	-

Table note:

Corresponding dates where a tropical cyclone was within 400km of Gladstone have been identified by the storms name.

11.3.6 Humidity

Dew point temperature is a measure of the amount of moisture available in the atmosphere; the higher the dew point temperature the higher the amount of water vapour present. Figure 11.23 shows the 9.00am and 3.00pm monthly mean dew point temperatures recorded at Radar Hill from 1957 to 2010. The determination of mean daily diurnal humidity on a monthly basis, for Radar Hill, was discontinued post-2010. There is very little diurnal variability between the two measures with the afternoon dew point being slightly higher on average. The seasonal variation is very evident with dew point temperatures dropping to below 10°C in July compared to 21°C in January. This pattern is typical of a sub-tropical location where the amount of moisture in the atmosphere sees an increase during the summer months as the Australian monsoon begins to form in the north. The data quality of the dew point observations does not allow further analysis of the ENSO/PDO phase interaction.

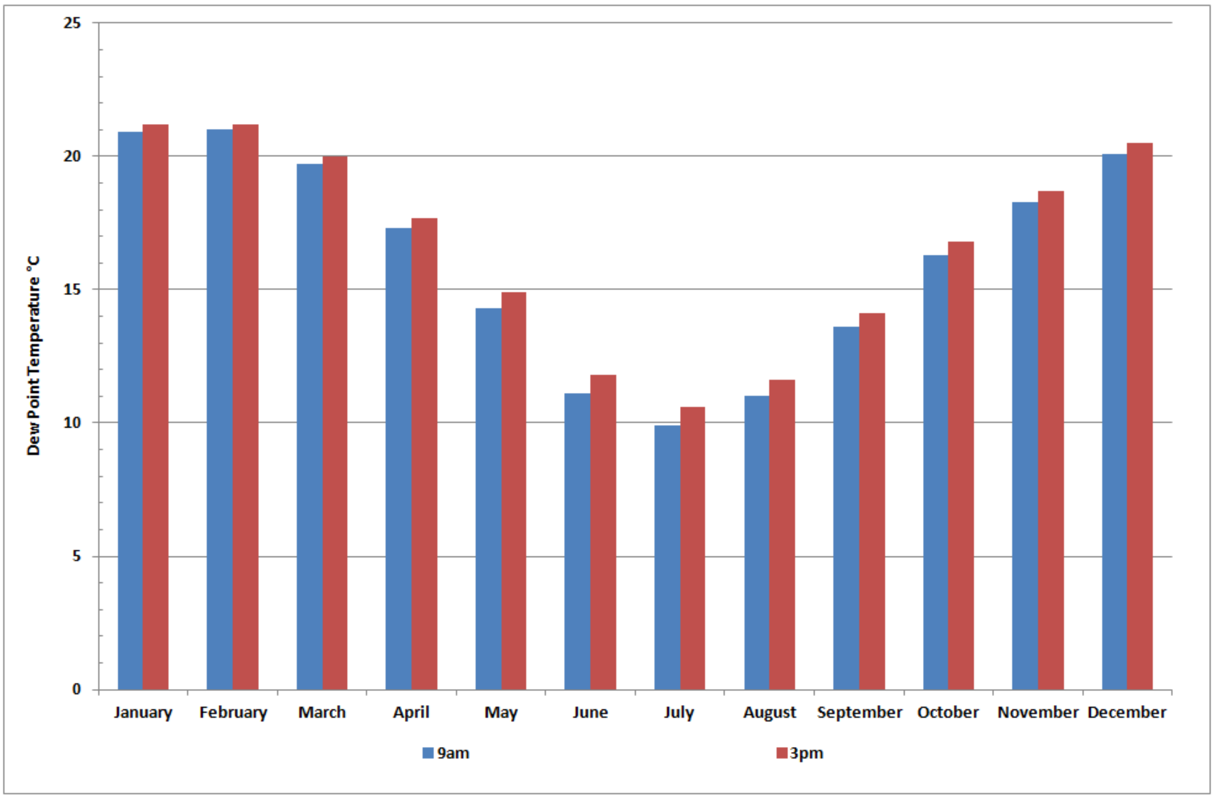

Figure 11.23 Monthly mean dew point temperature at 9.00am and 3.00pm at Radar Hill 1957 to 2010

11.3.7 Tropical cyclones

The International Best Track Archive for Climate Stewardship (IBTrACS: Knapp et al. 2010) is a global archive of all tropical cyclone tracks from 1897 to 2017. It is updated annually with the best estimate of each individual storm track across all Ocean Basins. The analysis presented here uses a subset of the IBTrACS archive for the South Pacific Basin and East Australian sub basin. The dataset was refined to eliminate those events that would not have a direct impact of the weather and climate of Gladstone the dataset was subset to only identify tropical cyclones whose path approached within a 400km radius of Gladstone. The analysis identified 118 tropical cyclones covering the period from 1908 to 2018.

On average 1.1 tropical cyclones can be expected to pass within 400km of Gladstone per year. However, this can range from zero to a maximum of seven, as was experienced in 1963 (refer Figure 11.24). The majority of tropical cyclones occur during the tropical cyclone season (1 November to 30 April); however tropical cyclones have occurred in May, June and July (refer Figure 11.25).

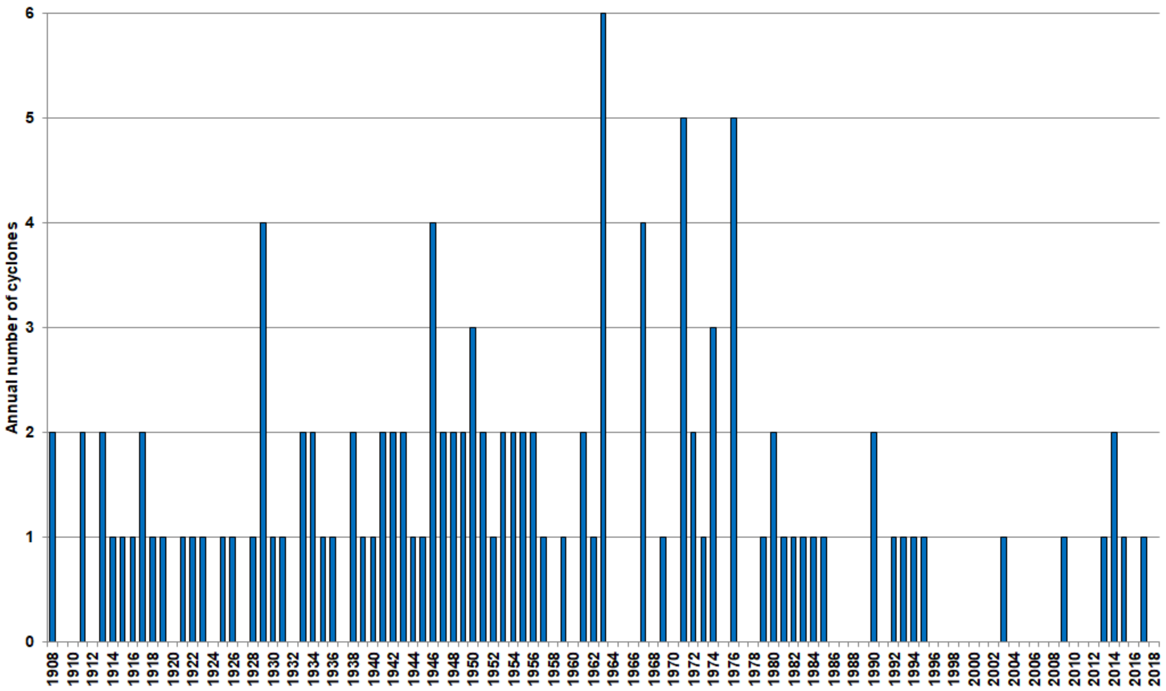

Figure 11.24 Annual total number of tropical cyclones that passed within 400km of Gladstone for the period 1908 to 2018

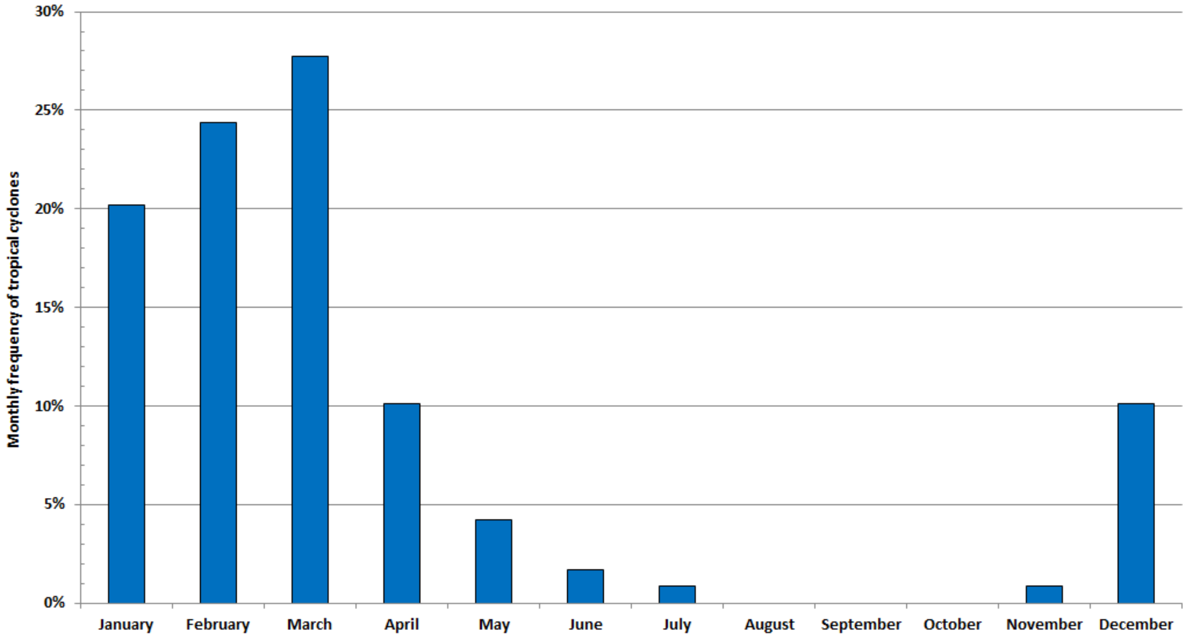

Figure 11.25 Monthly frequency of tropical cyclones that passed within 400km of Gladstone for the period 1908 to 2018

11.3.7.1 El Niño–Southern Oscillation/Pacific Decadal Oscillation tropical cyclone

Table 11.11 shows the frequency of tropical cyclones passing within 400km of Gladstone for the period 1908 to 2017 by ENSO and PDO phases. The data shows that there is a higher frequency of tropical cyclones during La Niña periods than El Niño periods. The influence of the PDO is shown in the increase in tropical cyclone frequency during Cool PDO/La Niña from 34% to 44% and the decrease in frequency during Warm PDO/La Niña from 34% to 20%. Neutral ENSO is shown to have the highest frequency of tropical cyclone activity.

Table 11.11 **Tropical cyclone frequency within 400km of Gladstone from 1908 to 2017 by El Niño–Southern Oscillation and Pacific Decadal Oscillation phases**

Number of tropical cyclones within 400km of Gladstone	El Niño	La Niña	Neutral
1908 to 2018	14%	34%	53%
Cool phase PDO	10%	44%	46%
Warm phase PDO	20%	20%	60%
Undefined	14%	14%	71%

11.3.8 Sea level rise and wave height

According to the BoM State of the Climate report (BoM 2014), observations indicate that sea level rise has been occurring gradually since the 19th Century with a more rapid increase observed in the 20th Century. By 2012 the measured Global Mean Sea Level was 225mm (± 30mm) higher than in 1880, the earliest year for which robust estimates are available. The key contributors to sea level rise are thermal expansion due to ocean warming and melting of glaciers and ice sheets. From an Australia perspective, sea level rise can vary from region to region, with higher sea level rise observed in the north and rates similar to the global average observed in the south and east.

The ABSLMP managed by the BoM was established to monitor the sea level around the coastline of Australia. As indicated in Figure 11.26 the closest observation station to the Project area is located at Rosslyn Bay. Figure 11.27 provides a summary of monthly sea level measurements at the Rosslyn Bay observation station. Data available for Rosslyn Bay is over a relatively short time period from 1992 to 2017. Trends observed during this period are subtle and not easily identified, although an upward trend can be observed in the maximum monthly sea level indicator. Based on observations at Rosslyn Bay (MSQ 2018) the HAT is 5.14m LAT compared to Fisherman's Landing and Gladstone with HATs of 5.12m LAT and 4.83m LAT, respectively.

Extreme coastal sea levels caused by a combination of factors including astronomical tides, storm surges and wind-waves are exacerbated by rising sea levels. A major cause of storm surges along the coast of the East Coast cluster region are tropical storms and cyclones.

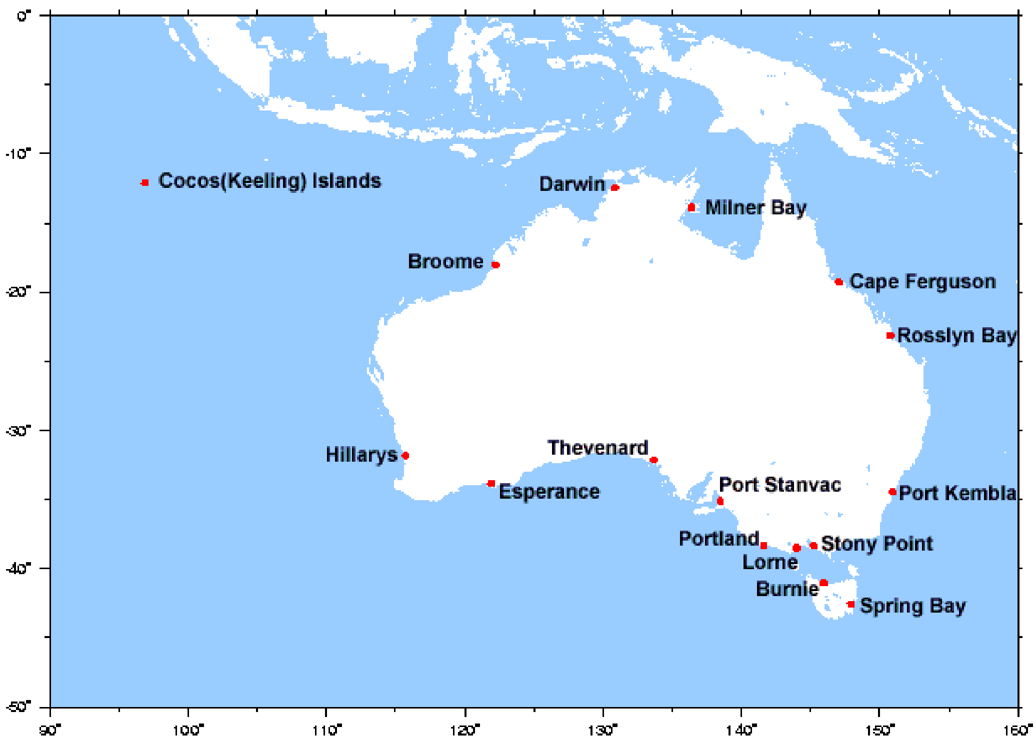

Figure 11.26 **Observation location for the Australian Baseline Sea Level Monitoring Project**

Source: BoM (2018a)

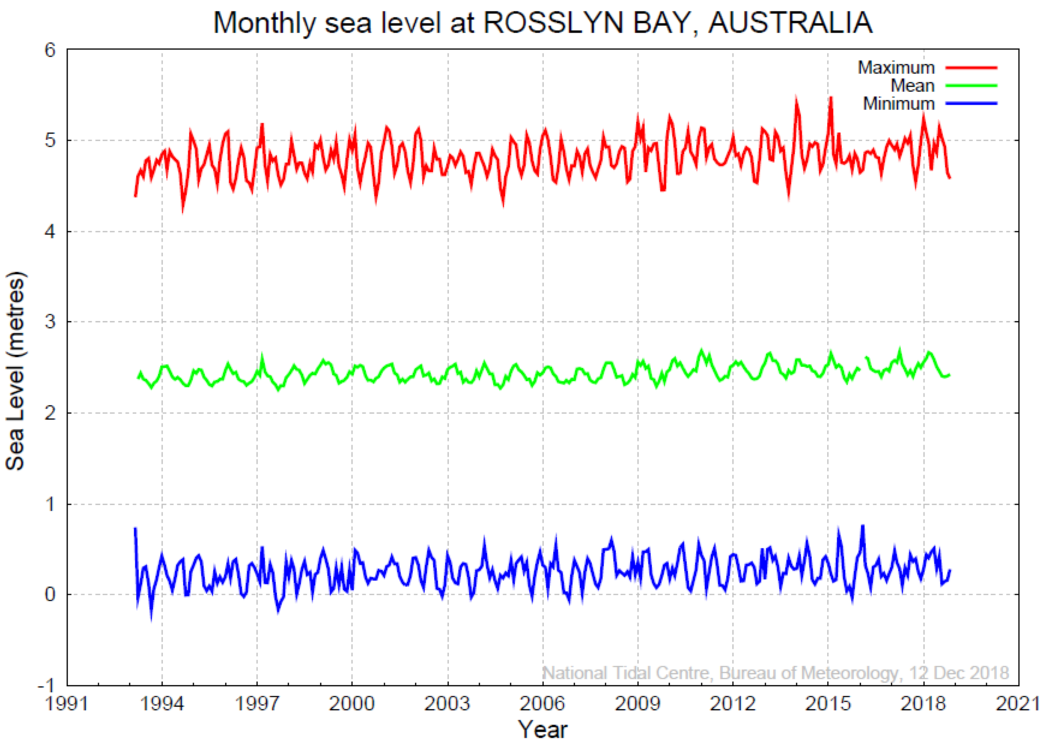

Figure 11.27 **Summary of monthly sea level rise at Rosslyn Bay**

Source: BoM (2018b)

11.4 Climate change

11.4.1 Climate projections

Greenhouse gas emissions scenarios provided by the IPCC serve as the basis for a number of global and regional climate models that simulate future conditions usually extending up to year 2100. These models were configured at a range of different temporal and spatial resolutions. A number of climate variables were modelled, though some variables may only be available from a subset of models.

The Coupled Model Intercomparison Project (CMIP) versions 3 and 5, known as CMIP3 and CMIP5, were used as the basis for the IPCC's Fourth and Fifth Assessment reports, respectively.

CMIP3 models are based on the SRES scenarios, which were developed to represent a range of possible future conditions based on greenhouse gas emissions with differing international or regional focuses on economic growth and/or environmental management. There were six scenario families identified, which were not associated with probability of occurrence. Therefore, none of the scenarios represent a best guess of the future. Figure 11.28 shows a plot of carbon dioxide (CO_2) emissions used as the basis for modelling. Further details about these scenarios can be found in the IPCC Fourth Assessment Report (IPCC SRES 2000).

CMIP5 models are based on the RCP scenarios developed for a range of greenhouse gas concentration (not emission) trajectories, which superseded the SRES scenarios. RCPs describe four possible climate futures, all of which are considered possible depending on how much greenhouse gases are emitted in the years to come. The four RCPs, RCP2.6, RCP4.5, RCP6, and RCP8.5, are named after a possible range of radiative forcing values in the year 2100 relative to pre-industrial values (+2.6, +4.5, +6.0, and +8.5 W/m2, respectively). Figure 11.29 shows a plot of CO_2 emissions and concentrations used as the basis for modelling. Further details about these scenarios can be found in the IPCC Fifth Assessment Report (IPCC 2014; van Vuuren et al. 2011).

A number of global climate models (GCM) and regional climate models (RCM) were developed based on the CMIP3 and CMIP5 scenarios. In addition to these, GCM and RCM data were further downscaled using dynamic or statistical techniques in order to improve on the native grid resolution. These include CSIRO's Conformal-Cubic Atmospheric Model (CCAM) (McGregor and Dix 2008) and the BoM statistical downscaling model (BoM-SDM) (Timbal and McAvaney 2001).

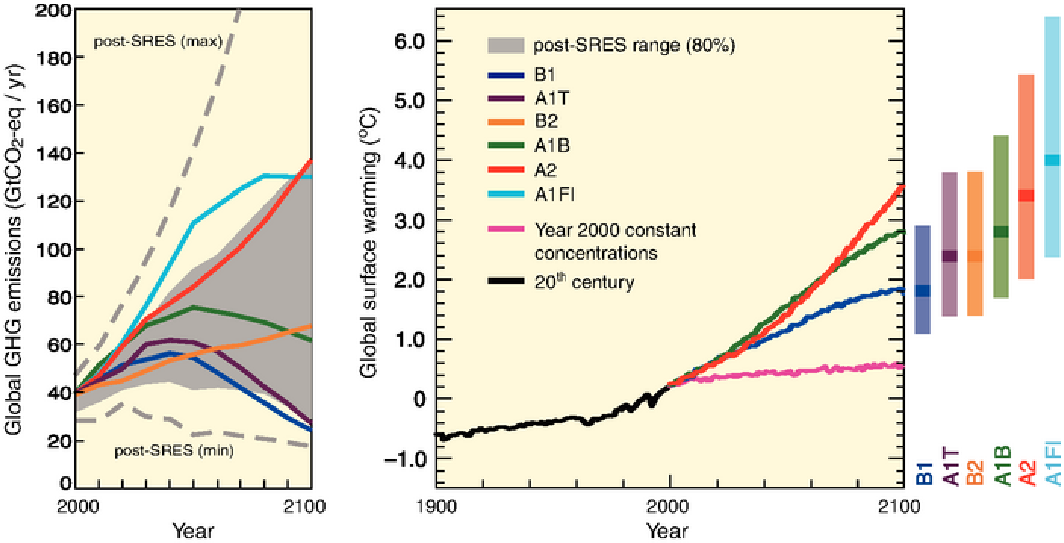

Figure 11.28 **Emissions of carbon dioxide (left) and associated surface warming associated with Special Report on Emissions Scenarios**

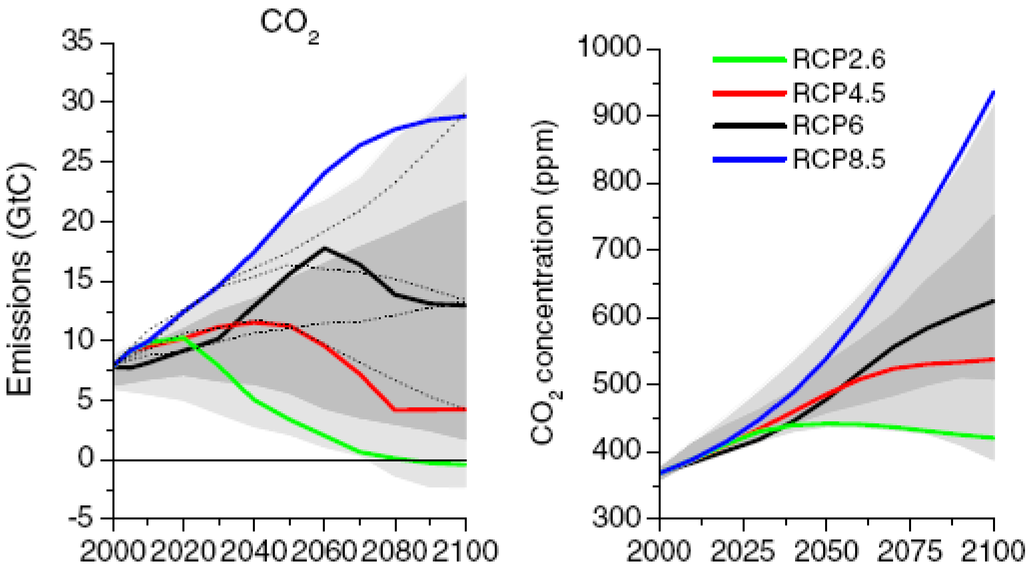

Figure 11.29 **Emissions of carbon dioxide across the Representative Concentration Pathways (left), and trends in concentrations of carbon dioxide (right)**

11.4.2 Climate change in Australia

CCIA is an online tool developed by the CSIRO that aims to assist user's understanding and application of climate change projections for impact assessment and adaptation planning.

CCIA includes tools that allow access to projections from global and regional climate models as well as statistically downscaled results. These models were developed for a number of greenhouse emission scenarios configured at a range of different temporal and spatial resolutions. CCIA provides different levels of access to users, ranging from simple graphs to more complex multi-dimensional analyses.

11.4.3 Climate Futures

The Climate Futures tool is part of the CCIA, which was built on CSIRO's Representative Climate Futures Framework (Clarke et al. 2011; Whetton et al. 2012).

Model data include outputs from model experiments CMIP5 and CMIP3. In addition to accessing the GCM data at the native grid resolution, data downscaled using dynamic or statistical techniques are also available.

Projected changes from the latest (CMIP5) models can be explored and accessed for 14 future time periods in 5 year increments from 2025 to 2090 for four scenarios of greenhouse gas emissions (RCP2.6, RCP4.5, RCP6.0 and RCP8.5). Data are available from up to 40 GCM, 6 CCAM and 22 BoM-SDM simulations.

Projections from the earlier (CMIP3) models are available for three future time periods (2030, 2055 and 2090) and three emissions scenarios (B1, A1B and A2). In this case, data are available from up to 18 GCM simulations.

Gridded GCM and downscaled model data were then grouped, analysed and presented based on Australia's diverse natural resources and NRM activities. There are eight NRM clusters identified, presented in Figure 11.30. Gladstone is located in the East Coast cluster, shown in navy blue (Dowdy et al. 2015), Gladstone is further classified as part of the East Coast North sub-cluster (Queensland side of the East Coast cluster) where more detailed analysis is available.

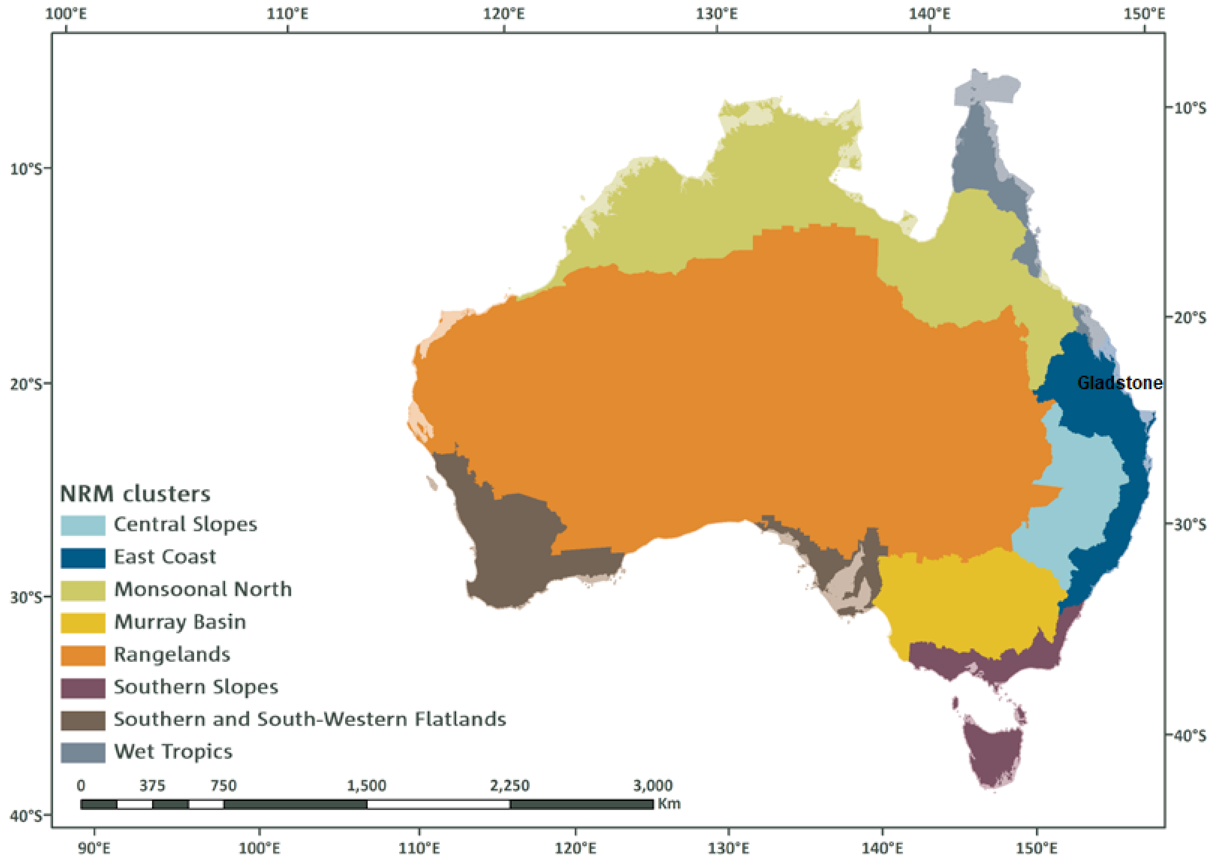

Figure 11.30 Natural resource management clusters

The Climate Futures tool offered the capability to analyse two variables simultaneously. However, analysis was constrained to one variable to facilitate discussion.

In addition to analysis on climate variables, data on model consensus are also provided. The tool also includes notes on suitability of specific models for a climate variable and a region.

The intermediate tool for climate futures also includes a scenario builder, wherein users can define the specific scenarios of interest. In addition to delivering these data, the tool also provides the most appropriate model to use for identified scenarios, as well as the most appropriate out of all the models with the greatest agreement on a range of predictions.

There are two levels of analysis built into the Climate Futures. The basic Climate Futures tool shows a summary of the number of models that predict a range of climate variables. This encompasses all models, regardless of the representativeness of the model. This information may be used to identify reliability of data as clustered consensus will indicate the ease of projection. On the other hand, a more distributed projection may suggest difficulty in predicting a certain variable.

The Projections Builder (intermediate Climate Futures tool) gives a range of climate projections based on models considered representative of the region. The tool also provides the specific models should the user decide to conduct a more comprehensive analysis.

11.4.4 Coastal and marine

Coastal and marine variables are available for selected points located within seven of the eight NRM clusters which included coastlines. Changes relative to the 1986 to 2005 baseline are available for the 30 year period centred on 2030 and 2090 for the sea surface temperature, sea surface salinity, ocean pH, aragonite saturation, sea level rise, and sea allowance.

11.5 Climate change assessment

11.5.1 Regional context

The change relevant to key climate variables were studied in a regional context by the working group 1 (WG1) of the IPCC (Christensen et al. 2013).

This section discusses the climate change on a regional scale, particularly temperature and precipitation changes, as well as tropical storms and cyclones changes.

11.5.2 Temperature and precipitation

Table 11.12 shows the temperature and rainfall projections for the East Coast North sub-cluster for 2030 and 2090. The results are generated from the area-mean temperature and precipitation deviations from the baseline climate period 1986 to 2005. The table shows the 25th, 50th and 75th percentiles, and the lowest and highest projections from the 42 models and the four RCP scenarios. The projections all converge on a warming climate with a significant decrease in average rainfall for all periods. On average the mean temperature is projected to rise by 1°C by 2030 for all scenarios. Worst case conditions projected for the mean climate of 2090 under RCP8.5 with an increase of 4 degrees of the annual average temperature.

Table 11.13 shows the summary of minimum and maximum temperature for RCP8.5 scenarios in the East Coast North sub-cluster.

Table 11.12 Summary of temperature and rainfall for Representative Concentration Pathways 8.5 scenarios in the East Coast North sub-cluster

Projection		Temperature (°C)		Precipitation (%)	
Season	Year	Median	Range	Median	Range
Summer	2030	0.9	(0.5 to 1.4)	-5	(-18 to 16)
	2090	3.7	(2.4 to 4.5)	-6	(-29 to 28)
Autumn	2030	1	(0.4 to 1.4)	-8	(-21 to 12)
	2090	3.6	(2.6 to 4.7)	-12	(-36 to 30)
Winter	2030	1	(0.6 to 1.4)	-10	(-34 to 14)
	2090	4	(2.8 to 4.8)	-17	(-49 to 18)
Spring	2030	1	(0.5 to 1.4)	-8	(-29 to 11)
	2090	3.7	(2.6 to 4.5)	-28	(-53 to 3)
Annual	2030	1	(0.6 to 1.3)	-6	(-17 to 8)
	2090	3.7	(2.5 to 4.7)	-16	(-32 to 17)

Table 11.13 Summary of minimum and maximum temperature for Representative Concentration Pathways 8.5 scenarios in the East Coast North sub-cluster

Projection		Temperature maximum (°C)		Temperature minimum (°C)	
Season	Year	Median	Range	Median	Range
Summer	2030	0.9	(0.5 to 1.6)	0.9	(0.4 to 1.4)
	2090	3.7	(2.6 to 4.7)	3.7	(2.3 to 4.7)
Autumn	2030	1	(0.3 to 1.3)	1	(0.5 to 1.3)
	2090	3.4	(2.6 to 4.8)	3.6	(2.5 to 4.8)
Winter	2030	1	(0.5 to 1.6)	1	(0.7 to 1.5)
	2090	3.9	(2.8 to 4.8)	3.9	(2.9 to 4.9)
Spring	2030	1.1	(0.5 to 1.5)	0.9	(0.6 to 1.4)
	2090	3.8	(2.7 to 5)	3.7	(2.5 to 4.5)
Annual	2030	1	(0.5 to 1.4)	1	(0.7 to 1.4)
	2090	3.6	(2.9 to 4.7)	3.7	(2.6 to 4.7)

11.5.3 Tropical storms and cyclones

Table 11.14 shows the projected change in frequency of tropical storms for the southwest Pacific. These were the results of a number of independent downscaling experiments that were conducted with various resolutions, initialisation models and downscaling models.

The ensemble mean projection for 2090 under RCP8.5 shows a reduction in tropical storm frequency in the southwest Pacific of 30%. The CSIRO contributed three model scenarios to these experiments all showing a consistent reduction in storm frequency of 27%, 33% and 38%. Only one experiment resulted in an increase in storm frequency (10%); however, the same model produced the largest decrease (90%) when initialised with a different model and grid resolution.

Table 11.14 Tropical storm frequency projections (%) for southwest Pacific for 2090 (Representative Concentration Pathways 8.5)

Model/type	Experiment	Grid res (km)	Tropical storm frequency projections (%)
CSIRO CCAM regional model nested in a suite of GCMs	A2 1990, 2090 GFDL CM2.1 MPI ECHAM5	15km	- 38
			- 33
			- 27
All 36 experiments	All	15km to 90km	- 30
JMA/MRI global AGCM timeslice	MIROC-H	60km	10
JMA/MRI global AGCM timeslice	CSIRO	20km	- 90

Table 11.15 shows the projected variation in intense tropical cyclones in the southwest Pacific. The ensemble mean shows a reduction in cyclone intensity of 17%. Interestingly the CSIRO contribution goes against the consensus with an increase of between 5% and 10%. The CSIRO Division of Atmospheric Research Limited Area Model (DARLAM) regional model also projected the largest increase of all the experiments of 26%. A similar experiment was undertaken for tropical cyclone/hurricane rainfall intensity. In this experiment all models show an increase in tropical cyclone precipitation between 2% and 15% globally; however, there were no experiments published for the southwest Pacific Basin.

In general, the results indicate a decrease in the formation of tropical cyclones. While the projection of increasing intensity of extreme rainfall events could indicate an increase in the intensity of tropical cyclones and extreme storms.

Table 11.15 Tropical storm intensity projections (%) for southwest Pacific for 2090 (Representative Concentration Pathways 8.5)

Model	Experiment	Resolution	Intense tropical cyclone frequency projections (%)
CSIRO CCAM regional model nested in a suite of GCMs	A2 1990, 2090 GFDL CM2.1 MPI ECHAM5	15km	5% to 10%
All experiments	All	15km to 90km	-17%
JMA/MRI global AGCM timeslice	Downscale CMIP3 multimodel ens. A1B change	V3.2 20km	-61%
CSIRO DARLAM regional model	3 × CO_2; 2061–2090 minus 1961–1990	30km	26%

11.5.4 East Coast assessment

The assessment for the East Coast is based on models that simulated the RCP8.5 scenario, which assumes a future with minimal mitigation of emissions, leading to rapidly rising CO_2 concentrations. The assessment considered the 30-day period centred at 2050. For climate variables where analyses are not available for 2050, data available for other periods were used.

11.5.5 Rainfall

Figure 11.31 is a graphical representation of the consensus of model rainfall predictions for the 2050 RCP8.5 scenario. This is based on all the models included in the database. The size of the bubbles represents the number of models.

Figure 11.31 shows that most models predict little change to a decrease in annual rainfall. Most models also predict little change to drier conditions during summer and autumn. During winter, most of the models predict drier to much drier conditions. Model predictions for spring rainfall are evenly distributed, ranging from much drier to wetter conditions.

Figure 11.32 shows the range of rainfall predictions based on models that are representative of the region for the 2050 RCP8.5. The consensus of the representative models is a general trend of decrease in rainfall throughout the year, which is most pronounced during spring.

Models representative of the region predict that annual rainfall could increase by 1% or decrease by approximately 25%, with maximum consensus predicting a 7% decrease in annual rainfall. Changes in autumn, winter, and spring rainfall range from a slight increase (2% to 12%) to a significant reduction (29% to 38%). Projections of the change in summer rainfall range from an increase of 8% to decrease of 17%.

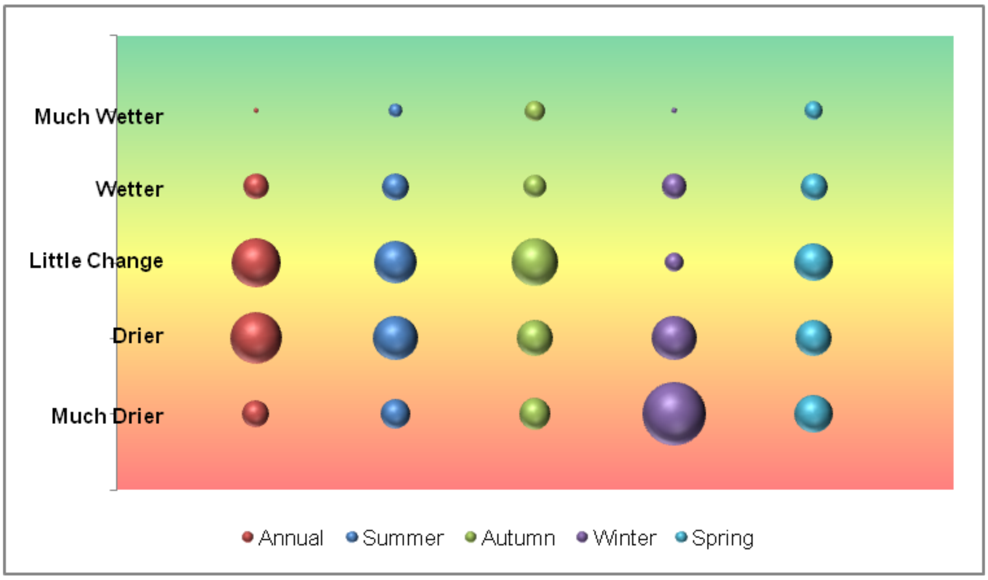

Figure 11.31 Consensus of all models with respect to change in rainfall (size of bubbles reflects the number of models)

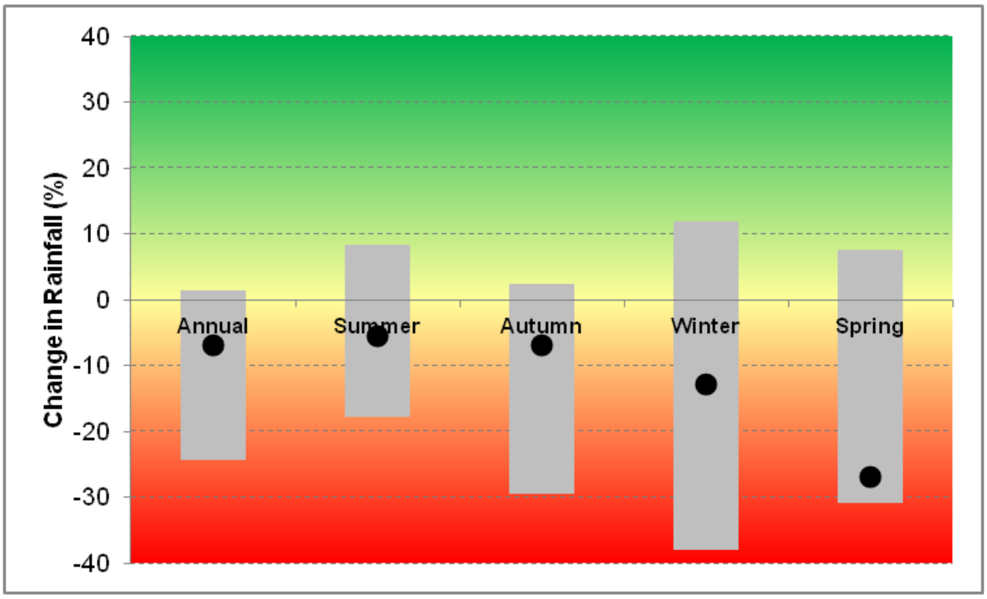

Figure 11.32 Predicted change in rainfall (Dots represent maximum consensus of representative models)

11.5.5.1 1-in-20 year rainfall

In a warming climate, extreme weather events are expected to increase in magnitude mainly due to a warmer atmosphere being able to hold more moisture. Figure 11.33 shows the range of change in frequency of extreme rainfall (1-in-20 year) as predicted by all models. Figure 11.33 shows a distinct consensus for prediction of little change to small increase during summer. The models show less agreement during autumn. Winter and spring also shows a strong agreement with more models predicting little change. However, there are also a number of models predicting a slight decrease in the occurrence of extreme rainfall during spring.

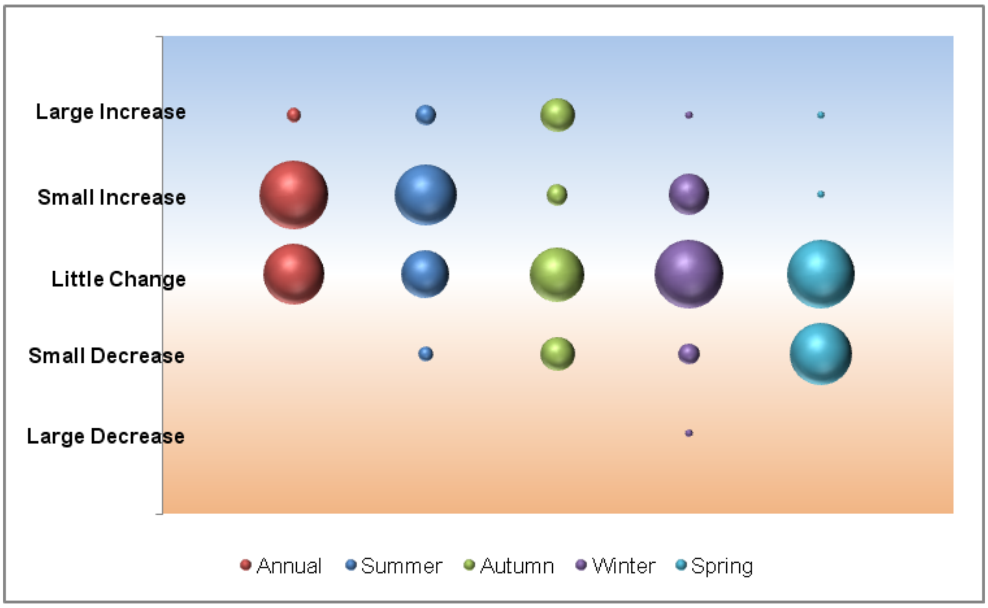

Figure 11.33 Consensus of all models with respect to change in frequency of 1-in-20 year rainfall (size of bubbles reflects the number of models)

11.5.5.2 Temperature

The consensus of all models on temperature prediction for the 2050 RCP8.5 scenario is shown in Figure 11.34, which shows that most models predict hotter temperature conditions in the future regardless of season.

Figure 11.35 shows the range of predicted temperature based on models that are representative of the region, which shows that all the models predict an increase in temperature, which is most pronounced during spring.

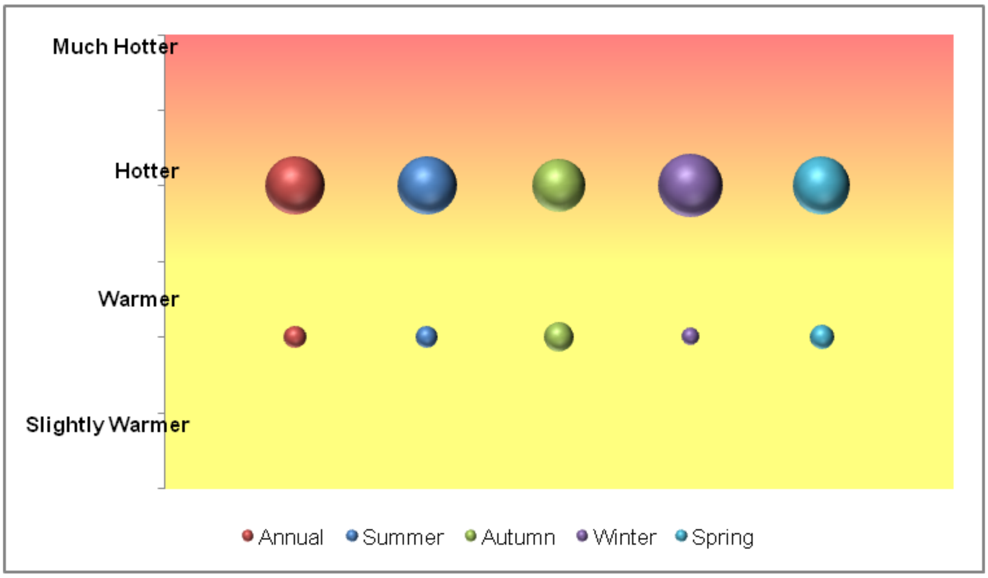

Figure 11.34 Consensus of all models with respect to change in temperature (size of bubbles reflects the number of models)

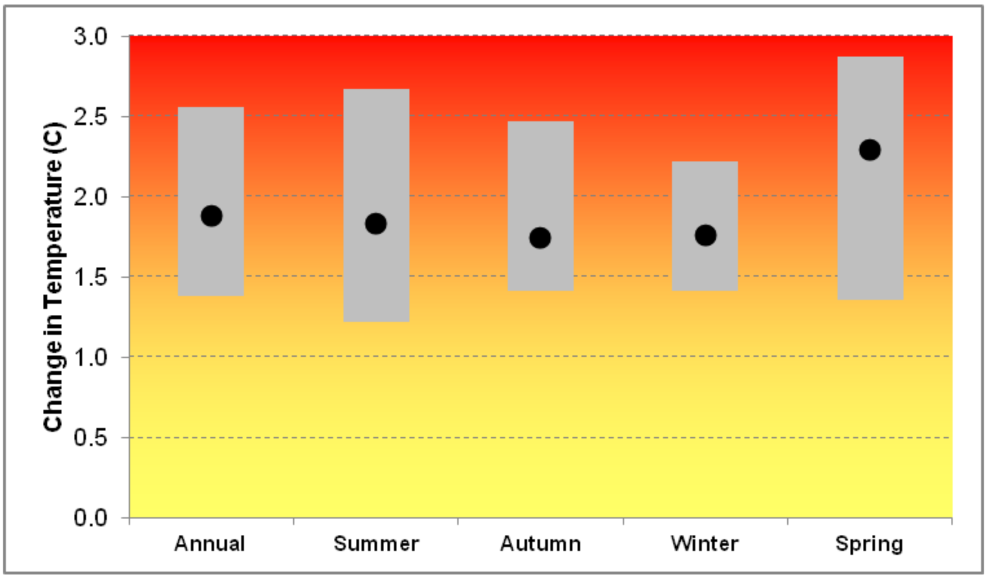

Figure 11.35 Predicted change in temperature (dots represent maximum consensus of representative models)

11.5.5.3 Wind speed

The consensus of all models on wind speed prediction for the 2050 RCP8.5 scenario is shown in Figure 11.36. The complexity of predicting changes to annual wind speed is evident in the relatively even distribution of model consensus. However, seasonal consensus seems to be clearer. In particular, there seems to be greater model agreement in the prediction of changes to mean summer and spring wind speeds. The confidence in projections of increases wind speed is relatively low.

This is also evident upon analysis of data extracted from models that are representative of the region, shown in Figure 11.37, which shows that while the models representative of the region predicted a range of wind speeds, most models agree on a projected increase in the upper range during summer, autumn, and winter. There is greater variability in the prediction of spring wind speed change.

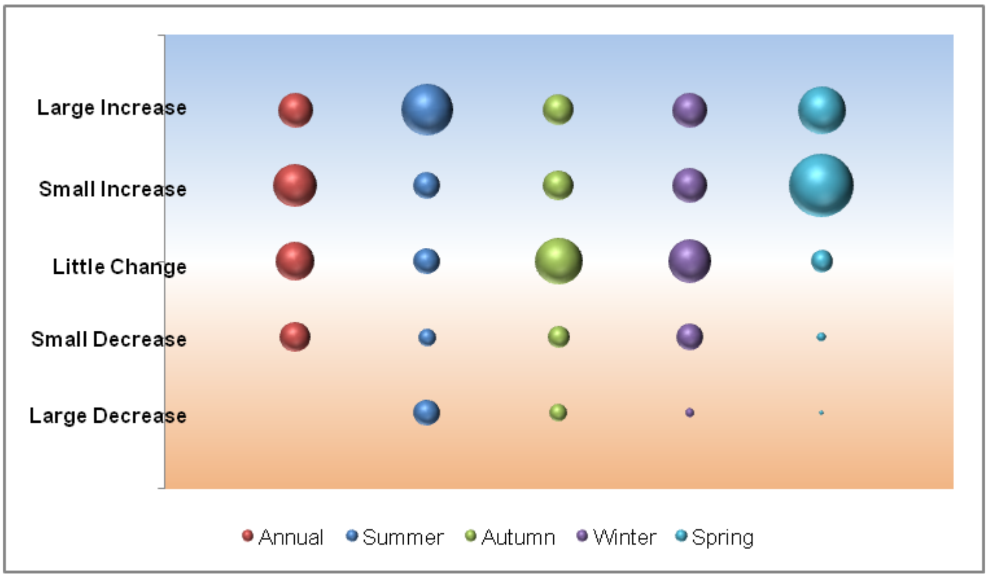

Figure 11.36 Consensus of all models with respect to change in wind speed (size of bubbles reflects the number of models)

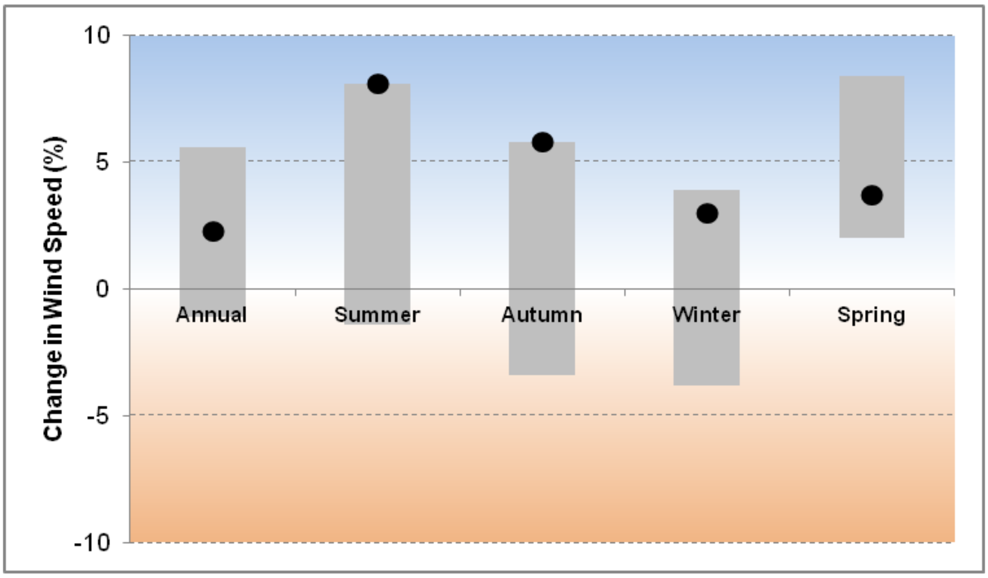

Figure 11.37 Predicted change in wind speed (dots represent maximum consensus of representative models)

11.5.5.4 1-in-20 year wind speed

The consensus of all models on 1-in-20 year wind speed for 2050 RCP8.5 scenario is shown in Figure 11.38. There is a general consensus that there will be little change in the frequency of 1-in-20 year wind speeds events.

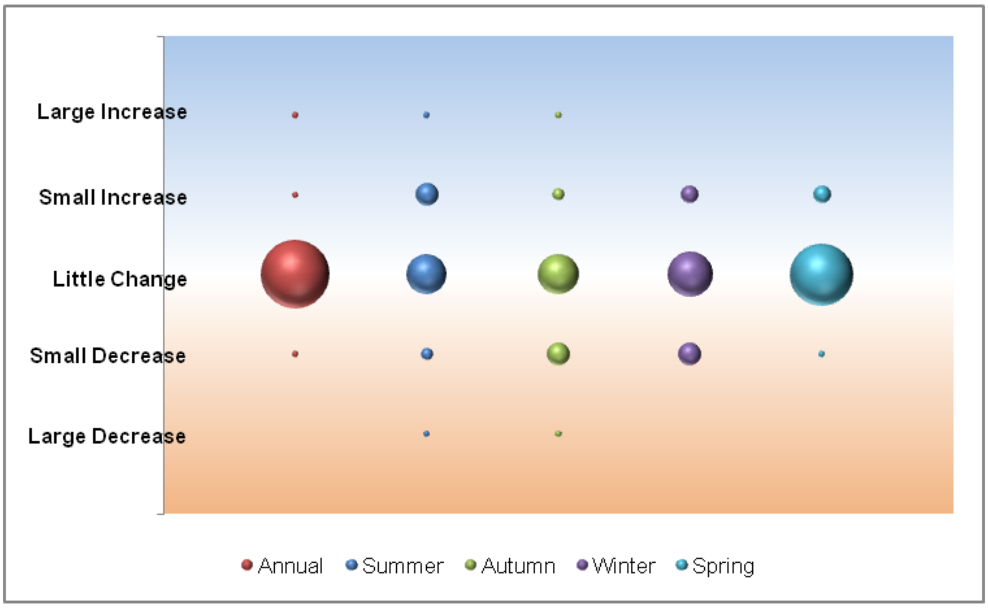

Figure 11.38 **Consensus of all models with respect to change in frequency of 1-in-20 year wind speed (size of bubbles reflects the number of models)**

11.5.5.5 Solar radiation

The consensus of all models on change in solar radiation for the 2050 RCP8.5 scenario is shown in Figure 11.39, which shows a distinct grouping of model predictions (i.e. little change and large increase), which could be attributed to the difficulty in predicting solar radiation.

Figure 11.40 shows the range of change in solar radiation based on models that are representative of the region. The general consensus of the representative models is a general trend of increase in solar radiation throughout the year, which is most pronounced during spring.

Models representative of the region predict that solar radiation could increase by less than 1% to less than 5%, with maximum consensus predicting a 1% increase. Changes in summer, winter, and spring range from a slight decrease (less than 2%) to a substantial increase (up to 8%).

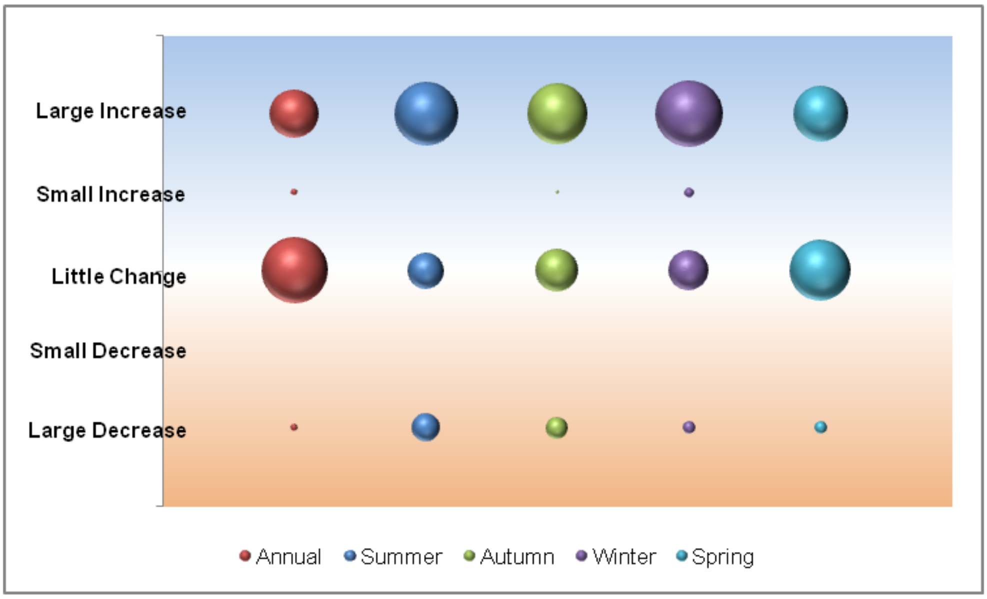

Figure 11.39 **Consensus of all models with respect to change in solar radiation (size of bubbles reflects the number of models)**

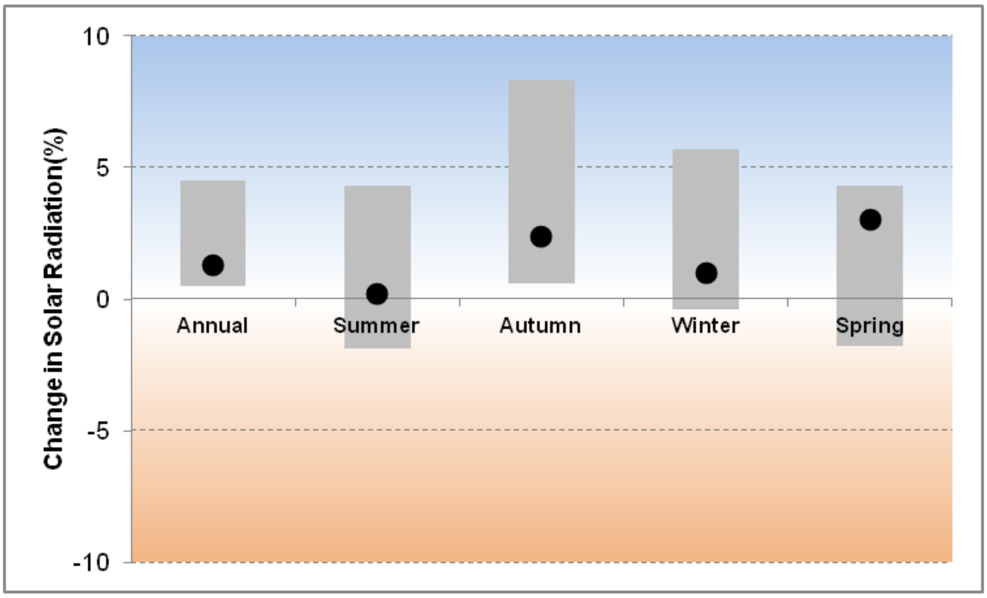

Figure 11.40 Predicted change in solar radiation (dots represent maximum consensus of representative models)

11.5.5.6 Humidity

The consensus of all models on change in humidity for the 2050 RCP8.5 scenario is shown in Figure 11.41, which shows that most models predict a small decrease in relative humidity.

Figure 11.42 shows the range of change in humidity based on models that are representative of the region. The general consensus of the representative models is a general trend of slight decrease in humidity throughout the year, which is most pronounced during spring. Spring is also shown to be the most variable out of all the seasons.

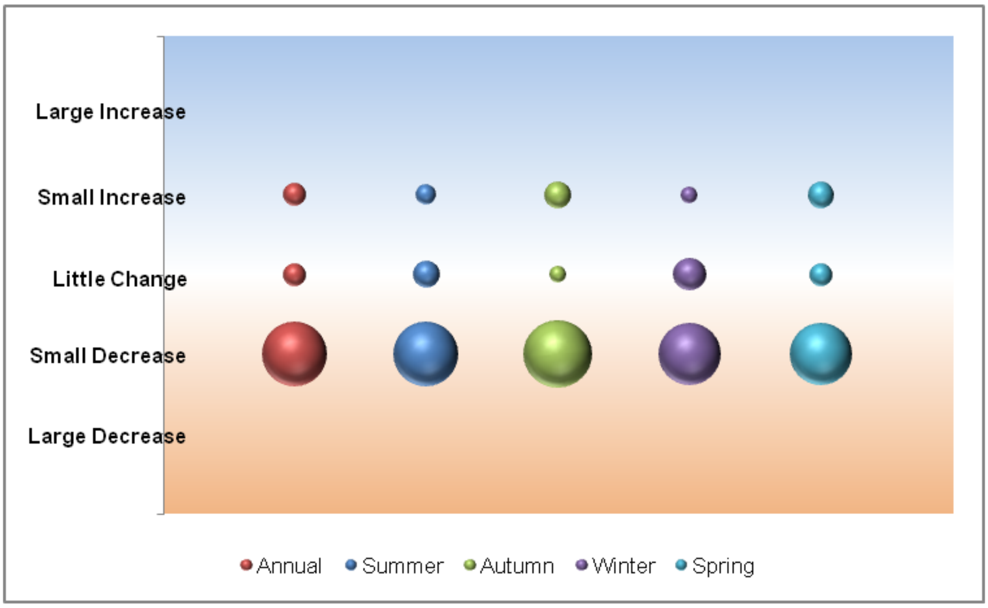

Figure 11.41 Consensus of all models with respect to change in humidity (size of bubbles reflects the number of models)

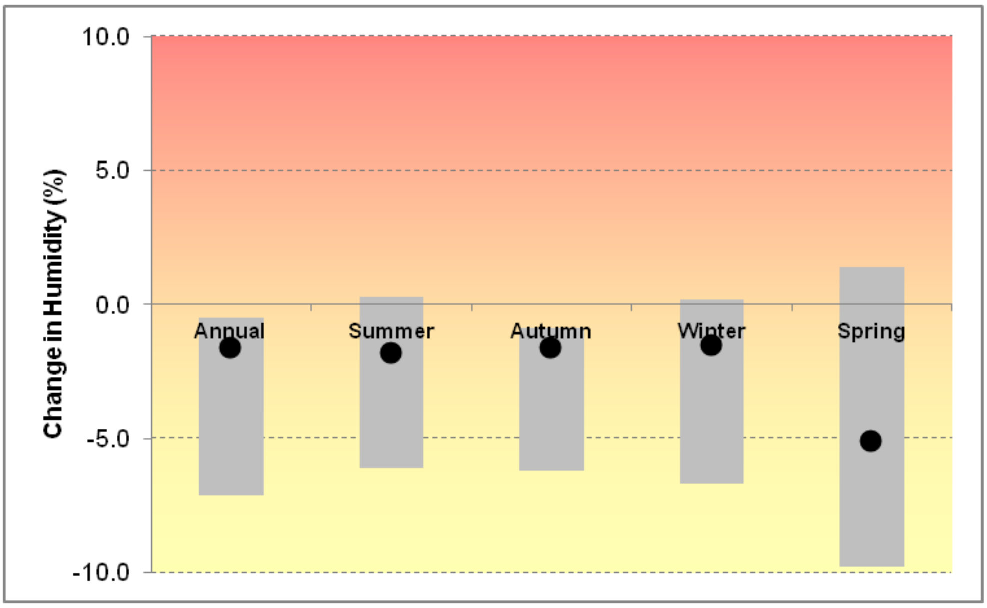

Figure 11.42 **Predicted change in humidity (dots represent maximum consensus of representative models)**

11.5.5.7 Sea level rise

Figure 11.43 shows the range of projected sea level rise based on models that are representative of the region. Relative to the 1995 to 2018 baseline, the projected sea level for 2030 is projected to increase by approximately 0.13m (0.005m/year). The 2090 sea level is anticipated to be 0.64m higher than the 1995 to 2015 baseline, indicating an accelerated increase of 0.0085 m/year.

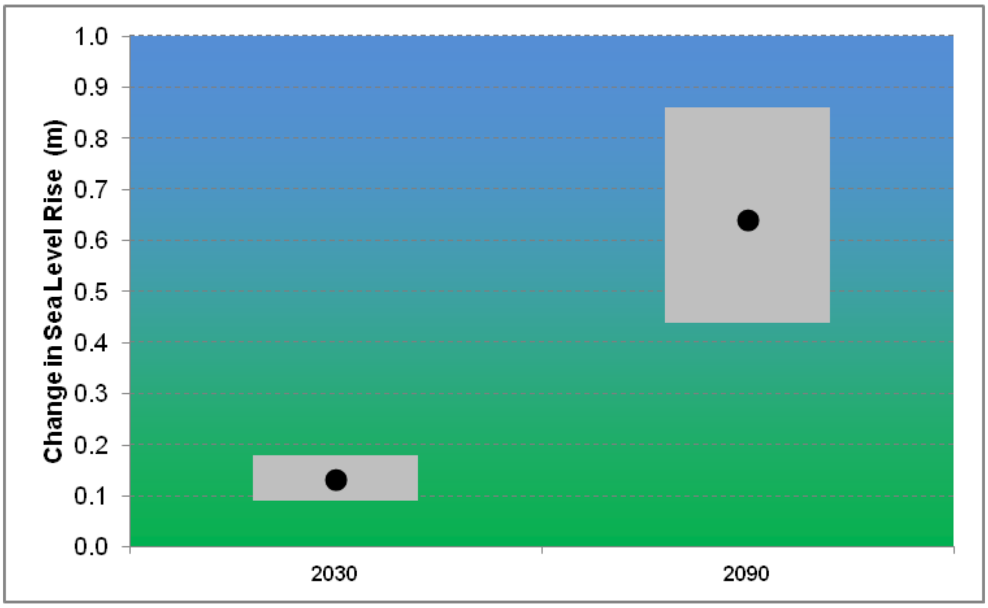

Figure 11.43 **Predicted change in sea level rise**

The consensus of all models on change in atmospheric pressure at sea level for the 2050 RCP8.5 scenario is shown in Figure 11.44, which shows that most models predict little change to a small increase during summer and autumn. The models show a more even distribution of predictions during winter and spring.

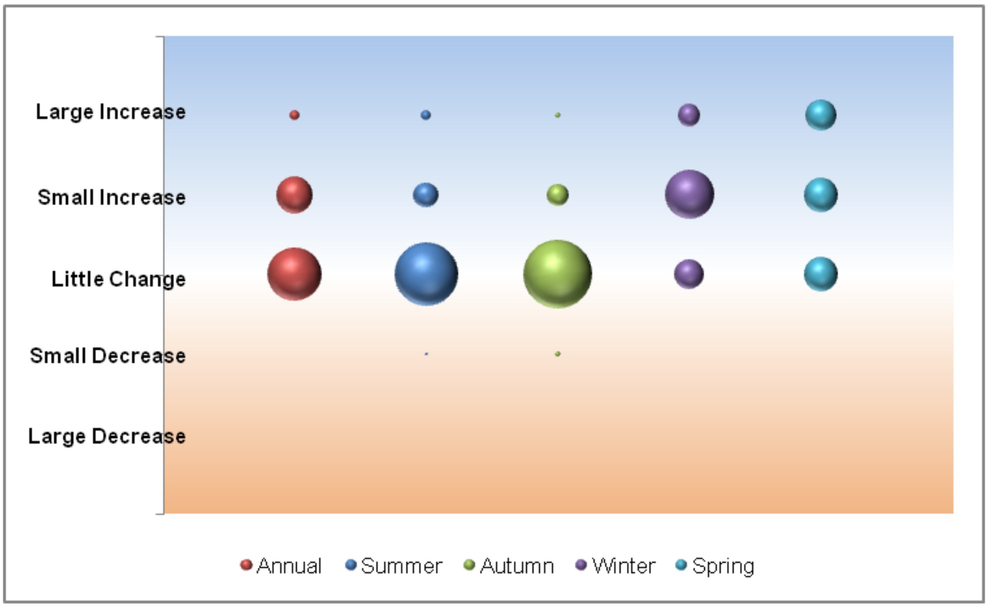

Figure 11.44 Predicted change in atmospheric pressure at sea level (dots represent maximum consensus of representative models)

Table 11.16 shows the range of change sea level as well as in other coastal and marine variables predicted for the East Coast for the years centred on 2030 and 2090.

Table 11.16 Range of model projections for coastal and marine variables

Variable	Units	2030	2090
Sea surface temperature	C	0.8 (0.5 to 1.0)	2.9 (2.1 to 3.5)
Sea surface salinity	g/kg	0.02 (-0.06 to 0.13)	-0.14 (-0.26 to 0.45)
Ocean pH	-	-0.08 (-0.08 to -0.07)	-0.14 (-0.26 to 0.45)
Aragonite saturation	-	-0.41 (-0.46 to -0.38)	-1.53 (-1.61 to -1.42)
Sea level rise	m	0.13 (0.09 to 0.18)	0.64 (0.44 to 0.86)
Sea allowance	m	0.14	0.78

The DTMR's guideline *Storm Tide – Issues for Design of Road Infrastructure in Coastal Areas* (DTMR 2014c) provides predicted storm surge and storm tide levels for a number of probability levels for future climatic conditions in the Gladstone area. The Gladstone predicted storm tide (i.e. tide, plus storm surge) and future climate change conditions included in the DTMR guideline are summarised in Table 11.17.

Table 11.17 Storm tide level data for Gladstone

Scenario		Storm tide level (m LAT)		
		100 year ARI	500 year ARI	1,000 year ARI
Gladstone (2003)	Storm tide level	5.09	5.78	6.07
	Storm surge allowance**	0.26	0.95	1.24
Gladstone (with future climate change conditions)*	Storm tide level	5.60	6.45	6.78
	Storm surge allowance**	0.77	1.62	1.95

Table notes:

* Based on Climate Change Scenarios for a 50 year planning period (DTMR 2014c)
** Assumes that the HAT at Gladstone is 4.83m LAT and AHD is 2.27m LAT (MSQ 2018)

11.5.5.8 Time in drought

The consensus of all models on projections of changes to frequency of time in drought is shown in Figure 11.45, which shows that most models predict a large increase in the length of droughts by 2090 under RCP 8.5.

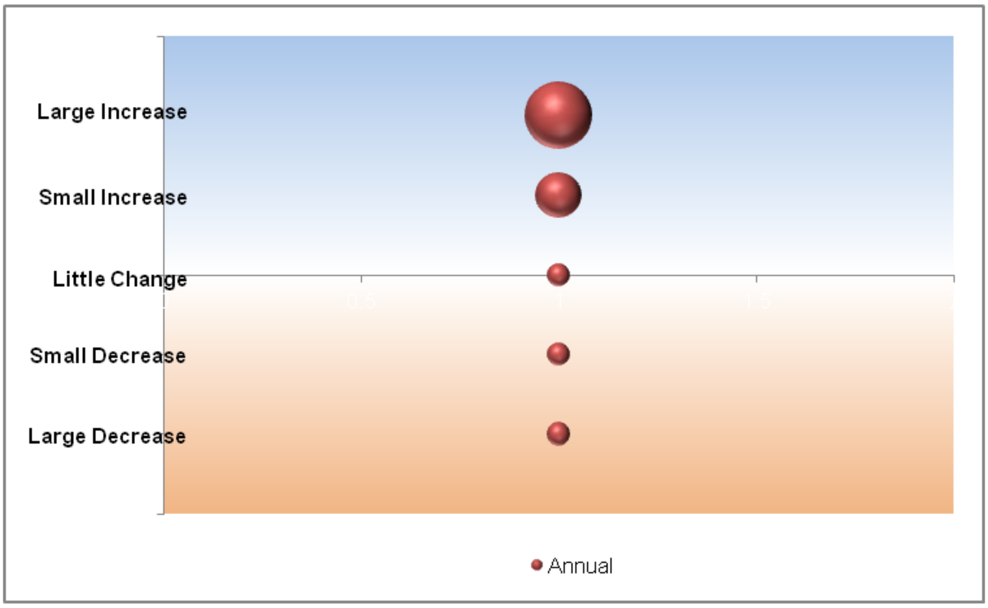

Figure 11.45 Consensus of all models with respect to change in frequency of time in drought (size of bubbles reflects the number of models)

11.5.6 Climate change summary

A summary of climate projections against existing conditions for each of the key climate variables with the potential to impact the Project is provided in Table 11.18.

Table 11.18 Summary of climate projections for key climate variables

Climate factor	Climate variable	Existing conditions	Climate change projections	Comments
Rainfall	Average annual rainfall	894mm	2050: -7% 2090: -16%	There is consensus that the average rainfall for Gladstone will experience little change or a minor decrease in the short term and a more pronounced decrease in the longer term
Extreme rainfall	Highest daily rainfall	254.4mm	Increase	There is high consensus that the intensity of heavy rainfall extremes will increase in the cluster, but the magnitude of change cannot be reliably projected. Extreme rainfall is generally associated with tropical storms and cyclones.
	Highest monthly rainfall	841.4mm		
Temperature	Daily mean temperature	24 to 30°C Summer	2030: +1.0°C 2090: +3.7°C	
	Daily maximum temperature	27 to 35°C Summer		
Wind speed	Seasonal mean	4 to 4.7m/s	Little or no change projected	
	Maximum wind gusts	82 to 156km/h	Little or no change projected	Maximum wind gusts are generally associated with extreme storms and frontal systems as well as cyclone events

Climate factor	Climate variable	Existing conditions	Climate change projections	Comments
Sea level	HAT (Fisherman's Landing)	5.12m (LAT)	2030: +0.14m 2090: +0.78m	
	Storm tide (Gladstone)	5.78m (LAT)	6.45m (LAT)	500 year ARI (refer Table 11.12)
Tropical storms and cyclones	Frequency	1.5 per year (average)	Decreased frequency Increased intensity	

11.6 Climate change impact assessment

11.6.1 Summary of potential impacts of climate change

Changing climate and weather patterns associated with climate change have the potential to impact on the construction and operational phases of the Project. Table 11.19 contains a summary of the potential impacts of climate change on the Project. The potential impacts on aquatic ecological communities and species from climate change (e.g. coral bleaching) which has the potential to occur at the same time as Project activities is provided in Section 21.4.5.

Table 11.19 Potential impacts of climate change on the Project by project phase

Climate factor	Design	Construction	Operational
Rainfall	No effect	No effect	Changes in soil moisture balance of reclamation area leading to movement and instability
Extreme rainfall	Overload of stormwater management system	Potential for delays in the construction schedule due to increased downtime Increase in erosion and sediment control measures More frequent discharges from the dredging dewatering process	Changes in soil moisture balance of reclamation area leading to movement and instability Potential increase of runoff and flooding Potential movement of sediment Potential impacts to water quality
Temperature	Future failure or fault of bund walls due to temperature tolerances of design and materials (e.g. road surfacing and concreting)	No effect in short term	Higher temperatures/evaporation leading to change in soil moisture and subsequent instability of the reclamation area and long term future land use outcomes
Windspeed	No effect	No effect	No effect
Sea level	Future inundation of reclamation area resulting in structural damage	No effect in short term	Infrastructure that does not take climate change into consideration may be less efficient or fail during the operational phase, including impacting on the long term future land use outcomes

Climate factor	Design	Construction	Operational
Tropical storms and cyclones	Future inundation or instability of reclamation area resulting in structural damage	Dredging equipment incident (e.g. collision or oil spill) Damage to bund walls and/or sheet piles or similar earth retaining structure Potential for delays in the construction schedule due to increased downtime	Infrastructure that does not take climate change into consideration may be less efficient or fail during the operational phase, including impacting on the long term future land use outcomes Damage to bund walls and/or sheet piles or similar earth retaining structure, and movement of sediment, and decrease in marine water quality Maintenance dredging equipment incident (e.g. collision or oil spill)

11.7 Mitigation measures

The following mitigation measures will be implemented during the Project activities to minimise potential climate change impacts on the Project:

- Detailed design of the BUF and WBE reclamation area to consider potential changed surface water volumes in extreme rainfall events
- Detailed design to consider the effects of increasing temperature on material selection for the BUF and WBE reclamation area bund walls
- Detailed design for the BUF and WBE reclamation area to include a ground stability assessment considering potential changes to temperature and rainfall profiles
- Site management plan will be prepared for the BUF and WBE reclamation area for the ongoing monitoring and management of ground stability
- Detailed design for the BUF and WBE reclamation area to consider extreme events. A detailed analysis of storm surge and climate change allowances will be undertaken during detailed design of the BUF and reclamation area bund walls. The EIS preliminary design for the BUF and bund walls has allowed for a combined storm tide and sea level change up to 7m LAT. This is a 0.55m allowance above the predicted 500 year ARI storm tide, including a climate change estimate of 6.45m LAT.
- Prepare and implement a cyclone management plan during Project activities
- Implement the findings and recommendations of the *Independent Review of the Bund Wall at the Port of Gladstone* (April 2014) (refer Appendix D).

11.8 Risk assessment

11.8.1 Methodology

To assess and appropriately manage the climate change risks which need to be addressed by the Project, a risk assessment process has been implemented (herein referred to as ‘risk assessment’). The risk assessment methodology adopted is based on principles outlined in the:

- AS/NZS ISO 31000:2009 Risk management – Principles and guidelines
- HB 203:2012 Handbook: Managing environment-related risk.

The risk assessment identifies and assesses the climate change risks to the Project for the establishment of the BUF and WBE reclamation area, dredging activities, installing navigational aids and operational management of the WBE reclamation area.

The purpose of this risk assessment is to identify potential climate change impacts to prioritise environmental management actions and mitigation measures, and to inform the Project decision making process.

The risk management framework incorporates the Australian/New Zealand Standard for Risk Management (AS/NZS 4360:2004) and contains quantitative scales to define the **likelihood** of the potential impact occurrence and the **consequence** of the potential impact should it occur.

An overview of the interaction between Project activities (drivers/stressors), sensitive values/receptors and the risk impact assessment process is provided in Figure 11.46.

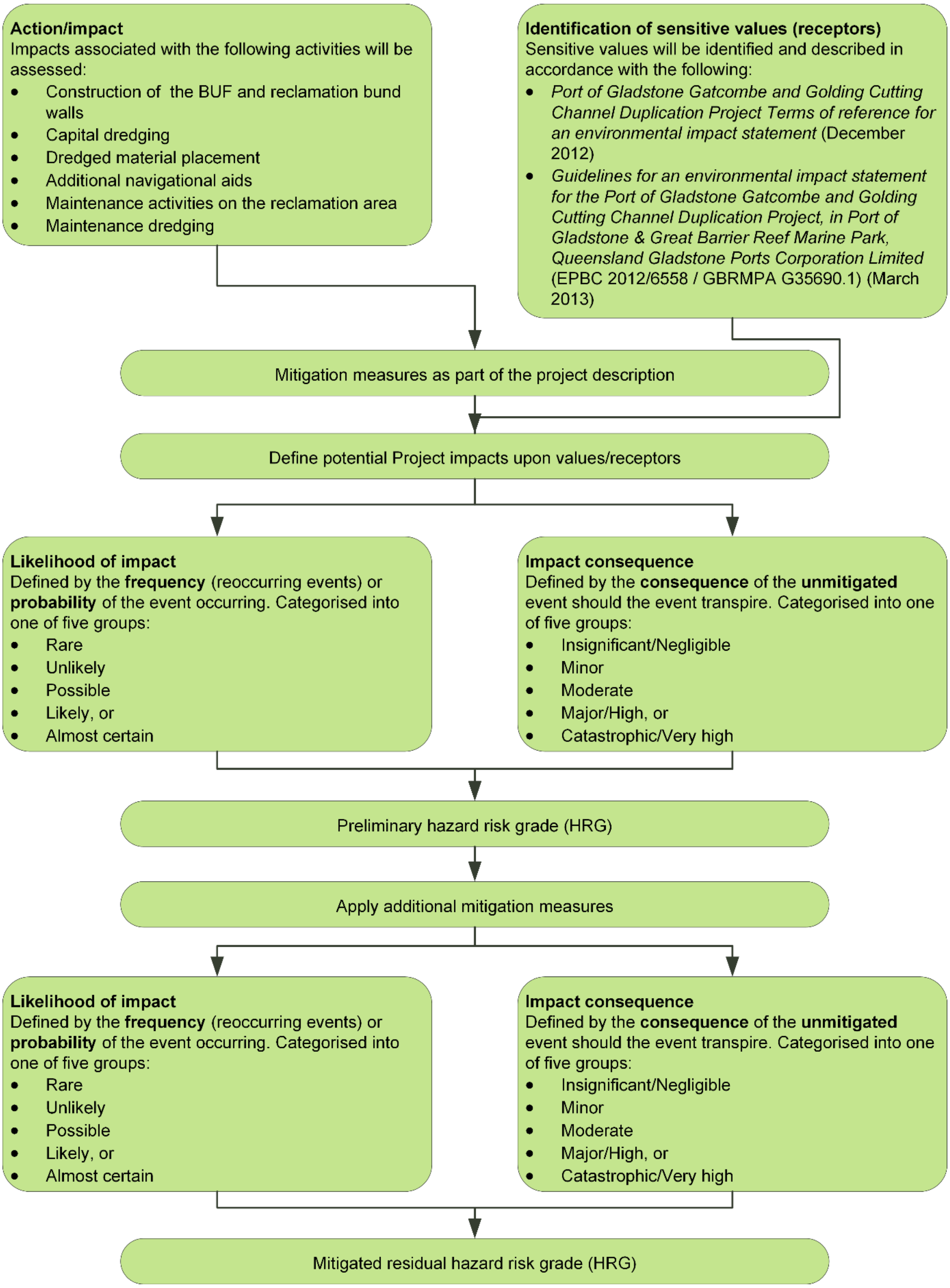

Figure 11.46 Risk assessment framework

Criteria used to rank the **likelihood** and **consequence** of potential impacts are provided in Table 11.20 and Table 11.21, respectively.

Table 11.20 Environmental (ecosystem), public perception and financial consequence category definitions (adapted from GBRMPA 2009)

Description	Definition/quantification[1]		
	Environmental*	**Public perception**	**Financial**
Negligible (Insignificant)	No impact or, if impact is present, then not to an extent that would draw concern from a reasonable person No impact on the overall condition of the ecosystem	No media attention	Financial losses up to $500,000
Low (Minor)	Impact is present but not to the extent that it would impair the overall condition of the ecosystem, sensitive population or community in the long term	Individual complaints	Financial loss from $500,001 to $5 million
Moderate	Impact is present at either a local or wider level Recovery periods of 5 to 10 years likely	Negative regional media attention and region group campaign	Financial loss from $6 million to $50 million
High (Major)	Impact is significant at either a local or wider level or to a sensitive population or community Recovery periods of 10 to 20 years are likely	Negative national media attention and national campaign	Financial loss from $51 million to $100 million
Very high (Catastrophic)	Impact is clearly affecting the nature of the ecosystem over a wide area **or** impact is catastrophic and possibly irreversible over a small area or to a sensitive population or community Recovery periods of greater than 21 years likely **or** condition of an affected part of the ecosystem irretrievably compromised	Negative and extensive national media attention and national campaigns	Financial loss in excess of $100 million

Table notes:

1 Quantification of impacts should use the impact with the greatest magnitude in order to determine the consequence category

* For Matters of National Environmental Significance (MNES) protected under the provisions of the EPBC Act the *Matters of National Environmental Significance – Significant Impact Guidelines 1.1 – Environmental Protection and Biodiversity Conservation Act 1999* (DoE 2013) are to be used to determine the consequence category

Table 11.21 Likelihood category definitions (adapted from GBRMPA 2009)

Description	Frequency	Probability
Rare	Expected to occur once or more over a timeframe greater than 101 years	0-5% chance of occurring
Unlikely	Expected to occur once or more in the period of 11 to 100 years	6-30% chance of occurring
Possible	Expected to occur once or more in the period of 1 to 10 years	31-70% chance of occurring
Likely	Expected to occur once or many times in a year (e.g. 1 to 250 days per year)	71-95% chance of occurring
Almost certain	Expected to occur more or less continuously throughout a year (e.g. more than 250 days per year)	96-100% chance of occurring

Once the likelihood and the consequence has been defined, determination of the HRG of the potential hazard will be determined through the use of a five by five matrix (refer Table 11.22).

Table 11.22 Hazard risk assessment matrix (adapted from GBRMPA 2009)

Likelihood	Consequence rating				
	Negligible (insignificant)	Low (minor)	Moderate	High (major)	Very high (catastrophic)
Rare	Low	Low	Medium	Medium	Medium
Unlikely	Low	Low	Medium	Medium	High
Possible	Low	Medium	High	High	Extreme
Likely	Medium	Medium	High	High	Extreme
Almost certain	Medium	Medium	High	Extreme	Extreme

Table note:
Hazard risk categories identified in Table 11.22 are defined in Table 11.23

Table 11.23 Risk definitions and actions associated with hazard risk categories (adapted from GBRMPA 2009)

Hazard risk category	Hazard risk grade definition
Low	These risks should be recorded, monitored and controlled. Activities with unmitigated environmental risks that are graded above this level should be avoided.
Medium	Mitigation actions to reduce the likelihood and consequences to be identified and appropriate actions (if possible) to be identified and implemented.
High	If uncontrolled, a risk event at this level may have a significant residual adverse impact on MNES, MSES, GBRWHA and/or social/cultural heritage values. Mitigating actions need to be very reliable and should be approved and monitored in an ongoing manner.
Extreme	Activities with unmitigated risks at this level should be avoided. Nature and scale of the significant residual adverse impact is wide spread across a number of MNES and GBRWHA values.

11.8.2 Summary of risk assessment.

The risk assessment framework developed for the Project was applied to the potential impacts of climate change on construction and operational activities as identified by Table 11.19. A summary of the risk assessment for climate change impacts together with proposed mitigation measures to manage risk to acceptable levels is provided in Table 11.22. In general, the potential impacts identified can be managed through a combination of design mitigation measures for extreme events and the implementation of the Project EMP, Dredging EMP, site management plan (ground stability), and cyclone management plan.

Risk is the likelihood of disaster or hazard. This probability is implied to occur to an asset or a resource. In determining risk, mitigation measures could be implemented in order to reduce the likelihood of risk.

The risk associated with the potential impacts of climate change variables on the Project was assessed using the risk assessment methodology provided in Section 11.8.1.

Table 11.24 Potential climate change impacts and risk assessment ratings

Potential impact	Project phase					Preliminary HRG			Post mitigation HRG		
	Reclamation area and BUF establishment	Dredging	Navigational aids	Demobilisation	Maintenance	Likelihood	Consequence	HRG	Likelihood	Consequence	HRG
Extreme rainfall, exacerbated by climate change											
Overload of stormwater management system, causes runoff and localised flooding	✓				✓	Possible	Low	Medium	Unlikely	Low	Low
More frequent discharges from the dredging dewatering process		✓				Possible	Moderate	High	Unlikely	Low	Low
Increase in average and seasonal temperatures											
Damage of outer BUF and/or bund walls due to exceeding heat tolerances of construction materials	✓				✓	Possible	Moderate	High	Unlikely	Low	Low
Instability of the final landform of the reclamation area and long term future land use outcomes					✓	Possible	Moderate	High	Unlikely	Low	Low
Increase in average and seasonal temperature profiles and decrease in annual rainfall											
Increased evaporation rates and annual rainfall leading to changes in the soil moisture profile resulting in instability and movement of the reclamation area	✓				✓	Unlikely	Low	Low	Unlikely	Low	Low
Sea level rise											
Future inundation of the BUF and reclamation area, and not providing long term beneficial land use outcomes	✓				✓	Possible	Low	Medium	Unlikely	Low	Low
Tropical storms and cyclones, increased intensity											
Dredging vessels and/or other Project equipment incident potential injury or death or damage to equipment	✓	✓	✓	✓	✓	Possible	Low	Medium	Unlikely	Low	Low
Damage of outer BUF and/or bund walls resulting in decrease in marine water quality	✓	✓			✓	Possible	Moderate	High	Unlikely	Low	Low

Potential impact	Project phase					Preliminary HRG			Post mitigation HRG		
	Reclamation area and BUF establishment	Dredging	Navigational aids	Demobilisation	Maintenance	Likelihood	Consequence	HRG	Likelihood	Consequence	HRG
Increased sediment load in the channel resulting in an increased requirement for maintenance dredging and associated costs					✓	Possible	Low	Medium	Unlikely	Low	Low
Tropical storms and cyclones, increased intensity and increase in sea level											
Damage to BUF and/or bund walls, and movement of sediment leading to potential decrease on surrounding water quality, time delays due to additional dredging and clean up requirements including additional costs	✓	✓			✓	Possible	Low	Medium	Unlikely	Low	Low

11.9 Summary

The climate change assessment has determined and quantified future climate conditions with respect to established baseline conditions. Climate change is determined by comparing outputs from global and regional models, as well as projections with established baselines for the period relevant to the Project.

Climate change was addressed on a regional scale to provide additional perspective to the projected local changes. A more localised assessment for Gladstone was conducted using the CSIRO online tool CCIA.

Sea level rise, rainfall and temperature were identified as the critical variables likely to be affected by climate change and, hence, these parameters formed the basis of the assessment. Other climate variables available from the dataset were also analysed and for extreme events were also presented, where available.

The assessment of climate change concluded that:

- Most models predict that average as well as seasonal rainfall is likely to decrease throughout the year
- Most models predict that there may be minor decrease in the frequency of extreme rainfall events; however, the intensity of extreme rainfall events is projected to increase
- Most models predict that temperature is likely to increase throughout the year. Based on the most representative model, seasonal temperature is likely to increase by approximately 1°C by 2030 and 3.7°C by 2090.
- The mean projection shows a reduction in tropical storm frequency in the Southwest Pacific of 30%
- Current sea level projections show an increase of 0.14m by 2030 and 0.78m by 2090. Sea water is also predicted to be slightly more acidic in the future. The rise in sea level is also expected to exacerbate storm tides and wave height.

The potential impacts of climate change on the Project in addition to the consideration of historical climate are related to:

- Short term:
  - Higher intensity tropical storms or cyclones causing delays to activities or in the worst instance injury or death
- Longer term:
  - Higher temperatures and evaporation rates, lower average rainfall, sea level rise and more intense storm/cyclone systems having the potential to impact on the structural integrity of the WBE reclamation area
  - More intense storm/cyclone systems causing increased sediment load resulting in a need for more frequent maintenance dredging.

The potential impacts of climate change have been taken into account in the preliminary design for the Project and further analysis will be undertaken at detailed design stage, particularly for the BUF and WBE reclamation area bund wall.